NASA TECHNICAL NOTE

NASA TN D-4150




# VOLUME ION PRODUCTION COSTS IN TENUOUS PLASMAS:

## A General Atom Theory and Detailed Results for Helium, Argon, and Cesium

*by John V. Dugan, Jr., and Ronald J. Sovie*

*Lewis Research Center*
*Cleveland, Ohio*

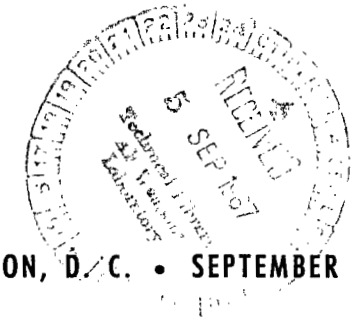


NATIONAL AERONAUTICS AND SPACE ADMINISTRATION • WASHINGTON, D. C. • SEPTEMBER 1967

NASA TN D-4150

# VOLUME ION PRODUCTION COSTS IN TENUOUS PLASMAS: A GENERAL ATOM THEORY AND DETAILED RESULTS FOR HELIUM, ARGON, AND CESIUM

By John V. Dugan, Jr., and Ronald J. Sovie

Lewis Research Center
Cleveland, Ohio

NATIONAL AERONAUTICS AND SPACE ADMINISTRATION

For sale by the Clearinghouse for Federal Scientific and Technical Information
Springfield, Virginia 22151 – CFSTI price $3.00

# VOLUME ION PRODUCTION COSTS IN TENUOUS PLASMAS: A GENERAL ATOM THEORY AND DETAILED RESULTS FOR HELIUM, ARGON, AND CESIUM*

by John V. Dugan, Jr., and Ronald J. Sovie

Lewis Research Center

## SUMMARY

A simple general theory for the volume ion production cost and ion production rate is presented for an arbitrary tenuous plasma having a Maxwellian distribution of electron energies. The ion production cost results are obtained by comparing the relative probabilities for the competing inelastic processes of excitation and ionization. The general theory treats a simplified atomic model and gives the volume ion production results for a general atom as a function of electron kinetic temperature. The results of this general theory are shown to be in good agreement with those of more detailed calculations for helium, argon, and cesium gases. These detailed results are obtained by considering the discrete atomic structure of the target atoms and are presented for two distinct cases: (1) a monoenergetic electron beam incident upon a cold neutral gas, and (2) the interaction of a thermal electron gas with cold neutrals. The semiclassical Gryzinski method was used to determine theoretically the cross sections needed for the general atom theory and the detailed argon and cesium studies. Experimental excitation functions were used in the detailed helium calculations. The Gryzinski technique for calculating cross sections is discussed, and the results of this theory are compared with available experimental data. This comparison shows that the Gryzinski method generally gives absolute cross sections that are good to within a factor of two or better. Its application should not introduce significant error in an eV/ion calculation, however, since the relative rates of the processes involved are of interest and not their absolute magnitudes.

---

*Portions of the calculations presented herein were presented at the 17th Gaseous Electronics Conference sponsored by the American Physical Society, Oct. 14-16, 1964 in Atlantic City, N.J. (See also NASA TM X-52064 1964) and at the 19th Gaseous Electronics Conference in Atlanta, Ga., Oct. 12-14, 1966.

# INTRODUCTION

In certain plasma devices operated at low pressures (e.g., Hall current accelerator, travelling magnetic wave accelerator, r-f discharges), it is useful to know the net energy cost for each ion produced in the plasma, the ion production rate, and the product of these terms which is the net power consumed in ion production. These quantities are necessary to perform calculations on steady-state power balance and species continuity for these systems. Specifically the ion production rate and the net power consumed in ion production are required to evaluate the inelastic collision terms in the macroscopic continuity and energy equations, respectively (ref. 1).

Since there are many methods of producing and maintaining laboratory plasmas and a wide range of operating pressures and energies, the ion production results for all plasma devices cannot be completely described. The applicability of this study is therefore limited in scope. It is confined to low pressure, optically thin plasmas with an elevated electron kinetic temperature. In low pressure plasma discharges the energy is generally added to the electrons and is then transferred to the other species by collisions. These collisions may be either elastic or inelastic; the former resulting in gas heating and the latter in excitation and ionization processes. In plasma production devices the electron energy is expended usefully if the atom is ionized but is lost if the target atom is excited and radiates away the excitation energy. In this sense a volume ion production cost may be defined that is generally applicable to these plasma devices and is independent of specific experimental configurations and boundary effects. Since in an actual experiment other loss mechanisms will be present, this definition constitutes only one term in the ultimate energy balance equation. This cost is obtained by comparing the relative rates for the competing processes of excitation and ionization. Such a cost will of course depend upon the distribution of electron energies in the plasma. Therefore, two plasma electron energy distributions are considered as limiting cases of ion production costs (1) a monoenergetic electron beam incident upon a cold neutral gas, and (2) a Maxwellian electron gas interacting with a cold neutral gas.

These costs could be straightforwardly calculated, if the cross sections for the various inelastic processes were known, by merely considering the collision frequency ratios for the processes of ionization and excitation. Ground state ionization cross sections have been obtained experimentally for most gases of interest; however, experimental ground state excitation cross section data are not generally available. This fact coupled with the complete lack of reliable inelastic cross sections for excited atomic states has seriously limited the calculation of ion production costs. This difficulty may be resolved, however, by use of the semiclassical Gryzinski (ref. 2) technique for calculating the needed cross sections.

The good agreement between the predictions of this method and the available experi-

mental cross sections indicate that this method can serve as a good approximation over a range of energy from inelastic threshold to several hundred electron volts. This method should be applied carefully, however, and the primary criteria for validity should be reliable experimental data, or, lacking this, the results of more refined quantum mechanical theory. Since ratios of the cross sections appear in the energy cost expression, it is sufficiently accurate if the theory predicts correct relative shapes for the excitation functions and not necessarily their correct absolute magnitudes.

Since it is desirable to do relatively simple calculations, the question of important excitations becomes a critical one. The number of important final states determines the atomic model to be used for the eV/ion calculation. In this respect, the use of the Gryzinski method is advantageous in that the cross section formulation affords a simple calculation of the volume ion production costs for a general atom. This general atom consists of the ground state and one effective excited state weighted for energy loss. The simple calculation is relatively accurate because the total excitation cross section is generally not very different from the sum of the individual excitation cross sections. Thus, consideration of a simplified atomic model thereby eliminates the detailed study of excitation to all possible allowed states of the atom.

In this note the volume ion production results for a general atom are obtained for the case of a Maxwellian electron gas interacting with a cold neutral gas. The results of this general atom theory are compared with those of detailed studies for argon, helium, and cesium gases. Detailed calculations for these gases have also been carried out for the case of a monoenergetic electron beam incident upon a cold neutral gas. Finally, there is a section devoted to a detailed critique of the semiclassical cross sections over the entire range of electron energies of interest.

## ION PRODUCTION EQUATIONS

### Assumptions and Limitations

The ion production cost calculated herein is based on the assumption that the sole energy loss mechanism for free electrons is inelastic collisions with ground state atoms (i. e., ionization and excitation of bound electrons). In the range of electron energies and temperatures of interest (from several to 50 eV), the energy loss in elastic collisions is clearly negligible. This is because the average fractional energy loss per encounter is small ($\Delta E/E \cong 2m_e/m_o \leq 5\times10^{-4}$) compared with the inelastic energy losses. (Symbols are defined in appendix A.) The results presented are applicable only to low pressure ($N_o \leq 10^{12}$ to $10^{14}$ $cm^{-3}$, $N_e \leq 10^{11}$ to $10^{12}$ $cm^{-3}$), partially ionized, optically thin plasmas for which cumulative inelastic impacts are improbable (i. e., tenuous plasmas

(refs. 3 and 4)). In this case, the collision frequencies for important excited state targets are considerably less than the corresponding radiative transition probabilities, which are of the order of $10^8$ seconds$^{-1}$ for the rare gases and $10^6$ seconds$^{-1}$ for cesium. A separate study has been conducted to investigate the effect of metastable atoms on ion production processes in a tenuous helium plasma and thereby to estimate the contribution of long-lived (electronic) excited states (ref. 5). These long-lived states will have a maximum effect in helium, and since this maximum effect was of the order of 25 percent in helium, they are not considered in the general atom theory.

Processes by which charged particles recombine may be considered separately in the ultimate power and species balance calculations. Low pressure discharges are primarily wall controlled, and for wall recombination this energy is considered as being lost from the plasma. This is a good approximation since the radiant flux from the wall to the plasma never becomes an important energy term even for low temperature plasmas. In partially ionized tenuous plasmas the energy released from radiative recombination also escapes from the plasma, and the rate at which this process populates electronic states remains negligible. There may be an energy feedback to the free electrons in three-body recombination and superelastic collisions, but these processes proceed at relatively low rates for the plasmas considered herein.

The monoenergetic beam study is a somewhat hypothetical limiting case which gives correct results for a beam incident upon a cold neutral gas. If the beam were impinging upon a plasma, however, the beam electrons may not collide directly with the neutrals, but could be thermalized by beam electron-plasma electron collisions or set up unstable plasma oscillations. These possibilities are considered in the discussion of this latter type of interaction in appendix B.

## Development of Equations

Monoenergetic beam case. - In this section, the equations necessary for determining the energy cost per ion will be developed for a monoenergetic beam of energy $E_B$ incident upon a cold neutral gas. Let the normalized probability that a beam electron of energy $E_B$ will produce an ion be called $P^+(E_B)$. The energy cost for each ion produced by the beam is then given by the relation

$$\varphi_B = \frac{E_B}{P^+(E_B)} \quad \text{eV/ion} \tag{1}$$

with the assumption that any excited state produced will lose the excitation energy by ra-

diation. In order to discuss the evaluation of the term $P^+(E_B)$, define the normalized probability for an inelastic collision with an energy loss $U_j$ as

$$P_j(E_B) = \frac{Q_j(E_B)}{Q_{tot}(E_B)} \tag{2}$$

where $Q_j(E_B)$ is the cross section for an inelastic collision with energy loss $U_j$ at the beam energy $E_B$ and $Q_{tot}(E_B)$ is the total inelastic cross section for the same beam energy. Furthermore, let the lowest energy level in the atom be represented as the $l^{th}$ state such that the minimum energy loss in an inelastic collision is $U_l$.

If the beam energy is such that $E_B - U_l \leq U_i$, then any electron that has an inelastic collision will not have enough energy left to cause an ionization. All the ions must therefore be produced by the first inelastic collision. The normalized probability for ionization in this case is given as

$$P_1^+(E_B) = \frac{Q^+(E_B)}{Q_{tot}(E_B)} \tag{3}$$

Thus in the case $E_B - U_l \leq U_i$, $P^+(E_B) = P_1^+(E_B)$.

If the free electron energies after the first collisions are greater than the ionization energy, cumulative probabilities must be included since these electrons may also produce ions. Consequently, in the range of beam energy from $E_B - U_l = U_i$ to $E_B - 2U_l \leq U_i$, $P^+(E_B)$ is given by the sum of the normalized probabilities for ionizing in either the first or second collision. Any electron in this energy range that has had two inelastic collisions will not have enough energy to ionize. In this case,

$$P^+(E_B) = P_1^+(E_B) + P_2^+(E_B) \tag{4}$$

where

$$P_2^+(E_B) = \sum_j P_j(E_B) P_1^+(E_B - U_j) \tag{5}$$

and the j indicates the summation over all inelastic processes including ionization.

As the beam energy is further increased to the limit $E_B - 3U_l \leq U_i$ one must consider the normalized probabilities for ionizing in either the first, second, or third collision in the calculation of $P^+(E_B)$. In this case,

$$P^+(E_B) = P_1^+(E_B) + P_2^+(E_B) + P_3^+(E_B) \tag{6}$$

where

$$P_3^+(E_B) = \sum_k \sum_j P_j(E_B) P_k(E_B - U_j) P_1^+(E_B - U_j - U_k) \tag{7}$$

and the k also indicates a summation over all inelastic processes. This procedure may be readily extended to higher beam energies by accounting for the additional ionization probabilities. The energy cost is calculated at each beam energy by substituting the appropriate $P^+(E_B)$ term into equation (1). In this treatment the calculations were terminated at a beam energy such that a maximum of three successive collisions were considered.

Maxwellian distribution case. - In this section the interaction between neutral gas atoms and a Maxwellian electron gas with an elevated electron kinetic temperature is analyzed. The theory is developed in the same manner as in reference 4.

The rate at which ground state atoms are raised to the $j^{th}$ excited state by monoenergetic electrons of speed $v_e$ is

$$\dot{N}_j(v_e) = N_o N_e Q_j(v_e) v_e \qquad cm^{-3}sec^{-1} \tag{8}$$

The cross sections employed, $Q_j$, are functions of electron speed $v_e$. (Q is generally represented as a function of incident electron energy $E_2$. However, when the collision coefficients are calculated, it is advantageous to express Q as a function of electron velocity $v_e$.) If there is a known distribution of free electron energies (Maxwellian, in this case), equation (8) becomes

$$\dot{N}_j = N_o N_e \langle Q_j(v_e) v_e \rangle \qquad cm^{-3}sec^{-1} \tag{9}$$

The bracketed quantity which represents the Maxwell averaged product of the cross section and electron velocity is the familiar collision coefficient in units of cubic centimeters per second. The rate at which energy is expended in excitation processes from the ground state is

$$\dot{E}_{j,\,ex} = \sum_j \dot{N}_j U_j = N_o N_e \sum_j \langle Q_j(v_e) v_e \rangle U_j \qquad eV/(cm^3)(sec) \tag{10}$$

Similarly, the rate of ion production in one-step ionization from the ground state is

$$\dot{N}_{ion} = N_o N_e \langle Q^+(v_e)v_e \rangle \qquad cm^{-3}sec^{-1} \tag{11}$$

where $\langle Q^+(v_e)v_e \rangle$ is the coefficient for ground state ionization. The rate at which energy is lost in this ionization process is given by

$$\dot{E}_{ion} = N_o N_e \langle Q^+(v_e)v_e \rangle U_i \qquad eV/(cm^3)(sec) \tag{12}$$

The net energy cost for producing singly ionized atoms is

$$\varphi_T = \frac{\dot{E}_{ion} + \dot{E}_{j,ex}}{\dot{N}_{ion}} \qquad eV/ion \tag{13}$$

which may be rewritten as

$$\varphi = U_i + \frac{\sum_j \langle Q_j(v_e)v_e \rangle U_j}{\langle Q^+(v_e)v_e \rangle} \qquad eV/ion \tag{14}$$

The net power consumed in ion production is simply the product of the ion production rate and the energy cost per ion. This power consumption is given by

$$\dot{W} = 1.602 \times 10^{-19} N_o N_e \langle Q^+(v_e)v_e \rangle \varphi \qquad W/cm^3 \tag{15}$$

In equations (8) to (15) it is assumed that ionization from excited states has little effect on the energy cost per ion (ref. 3).

## Cross Sections and Collision Coefficients

Experimental values. - The cross sections used in the helium calculations were those previously employed in reference 3. In this reference the results of a number of individual investigations of helium excitation cross sections were combined to yield a credible self-consistent set of helium excitation cross sections as a function of electron velocity. These excitation functions were multiplied by the electron velocity and averaged over a Maxwellian distribution of free electron energies to obtain the corresponding collision

coefficients. The argon and cesium cross sections used in the present treatment were calculated by using the semiclassical Gryzinski method.

Gryzinski theory - description, details of use, and limitations. - The Gryzinski cross section expressions were derived in a classical manner with the assumption that the inelastic electron-atom collision may be described purely as a two-body encounter between the incident and bound electrons. In the first approach to this problem (ref. 2) it was assumed that the bound electron had a single specified energy. Later refinement of the theory (ref. 6) incorporated the effect of variation in the bound electron energy by the distribution function $f(v) = (v/v_m)^3 e^{-(v/v_m)}$ where $v_m$ is the mean electron velocity. This choice of the form of $f(v)$ appears somewhat arbitrary and is inconsistent with distribution functions obtained from quantum mechanics. The assumption is not critical within the framework of the approximation, however, and the main justification for use of the later Gryzinski expression throughout will be agreement with existing experimental data. Monoenergetic cross sections calculated by this technique are generally found to be in satisfactory agreement with experimental data. They also exhibit the proper behavior at high electron energies (i.e., $(\ln E_2)/E_2$ behavior for $E_2 >> E_1$ : $E_2$ = kinetic energy of incident electron and $E_1$ = kinetic energy of bound electron).

According to the Gryzinski formulation (ref. 6) the cross section for an inelastic electron atom collision with an energy loss equal to or greater than a value $U$ is given by

$$Q(U, E_2) = \frac{M\sigma_o}{U^2} g_Q\left(\frac{E_2}{U}, \frac{E_1}{U}\right) \quad cm^2 \tag{16}$$

where

$$g_Q\left(\frac{E_2}{U}, \frac{E_1}{U}\right) = \frac{E_1}{E_2}\left(\frac{E_2}{E_2 + E_1}\right)^{3/2}\left[\frac{U}{E_1} + \frac{2}{3}\left(1 - \frac{U}{2E_2}\right)\ln\left(2.7 + \sqrt{\frac{E_2 - U}{E_1}}\right)\right]\left(1 - \frac{U}{E_2}\right)^{(2E_1+U)/(E_1+U)} \tag{17}$$

For a one electron outer shell, $E_1$ is equal to the ionization potential $U_i$. The symbol $M$ (eq. (16)) denotes the number of equivalent electrons (same principal and azimuthal quantum number) in the outer shell of the target atom. The target atom is considered to be in the ground state unless specified otherwise; $M$ serves as an effective probability factor which accounts for the number of target electrons most likely to undergo

inelastic energy transfer. For atoms with $M > 1$, the quantity $E_1$ should be calculated to be the mean energy required to remove all of the outer shell electrons. However, the choice of $E_1$ is only critical in the case of low temperature plasmas since its most significant effect is upon the slope of the cross section near threshold (ref. 7). For convenience $E_1$ will be taken as the ionization potential $U_i$ throughout this study as was done in references 7 and 8.

In the special case of ionization the threshold energy loss $U = U_i$ and equation (16) may be written as

$$Q^+(U_i, E_2) = \frac{M\sigma_o}{U_i^2}\left(\frac{1}{x}\right)\left(\frac{x-1}{x+1}\right)^{3/2}\left[1 + \frac{2}{3}\left(1 - \frac{1}{2x}\right)\ln\left(2.7 + \sqrt{x-1}\right)\right] \tag{18}$$

where $x = E_2/U_i$ is the dimensionless incident electron energy.

The Gryzinski formulation is particularly amenable to calculation of the ionization cross sections. The ionization expression considers only the possibility of an energy loss equal to or greater than a certain value $U = U_i$ to a continuum of free energy states. The upper limit on the energy transfer in the collision is merely that of the incident electron $E_2$. If one wishes to calculate the cross section for excitation to a discrete atomic level, the arrangement of the bound electronic levels which may be reached in the collision must be considered. However, the quantum mechanical structure of the target atom was not explicitly accounted for in the purely classical derivation of the cross section expressions. Thus, there is no formalism available for the straightforward treatment of the various types of discrete atomic excitations. Certain rules have therefore been adopted in this investigation on the basis that the results obtained show good agreement with the available experimental data (c.f., appendix C).

In order to clarify the discussion of excitation to discrete energy levels, it is necessary to distinguish between allowed (direct) excitations and other less likely excitation processes. An allowed excitation is an excitation to an atomic level which may also be reached from the initial state directly by the absorption of radiation (i.e., the selection rules $\Delta L = \pm 1$, $\Delta S = 0$ are satisfied). A forbidden excitation is an excitation to an atomic level for which a radiative excitation to the final state is optically forbidden (i.e., $\Delta L \neq \pm 1$ and/or $\Delta S \neq \pm 0$).

An additional aspect of electron-atom collisions which must be considered is that of the electron exchange process. Quantum mechanics allows for exchange of incident and bound electrons during collisions because of the required antisymmetry of the total wave function which has spin and space parts. This process may occur for interacting electrons with identical or different initial spins (i.e., singlet or triplet configuration). On the other hand Gryzinski has ignored spin considerations and oversimplifies the electron

exchange problem by considering the bound electron as initially residing in a potential well of height $U_i$. The incident electron can obtain enough energy in the atomic field to change places with the bound electron. The Gryzinski exchange cross section may be written as

$$Q_{exch}(U_n, E_2) = \frac{pM\sigma_o}{U_n^2}\left(\frac{U_{n+1} - U_n}{U_n}\right) g_{exch}\left(\frac{E_2}{U_n}, \frac{U_i}{U_n}\right) \quad cm^2 \tag{19}$$

where

$$g_{exch}\left(\frac{E_2}{U_n}, \frac{U_i}{U_n}\right) = \frac{U_n^2}{(E_2 + U_i)(E_2 + U_i - U_n)} \begin{cases} \dfrac{U_n}{U_i}\dfrac{E_2 - U_n}{U_{n+1} - U_n} & \text{if } E_2 < U_{n+1} \\ \dfrac{U_n}{E_2 + U_i - U_{n+1}} & \text{if } E_2 > U_{n+1} \end{cases} \tag{20}$$

and $p$ is an effective probability factor which will be discussed. In equations (19) and (20), $U_n$ and $U_{n+1}$ represent the energies of the state being excited and the cutoff state. The choice of these quantities will also be discussed in detail presently.

It should be noted that the exchange cross section should be added to the direct excitation expression in the case of an allowed transition since it is a competing process.

Now consider the general formulation for the calculations of excitation cross sections for discrete atomic states. The formulation for an allowed excitation will be used here for convenience. When the kinetic energy of the incident electron is above the excitation threshold for the state being considered (i.e., $E_2 > U_n$ where $U_n$ is the excitation energy) and below that of the next higher excited state of excitation energy $U_{n+1}$, the cross section is simply given by equation (17) with $U = U_n$. However, once the incident electron has enough energy to excite the level at energy $U_{n+1}$, excitation to this state competes with the excitation to the state at energy $U_n$. Then the cross section expression must become a difference function. Thus, the cross section expression for excitation to the state at energy $U_n$ is a measure of the probability of an excitation into the energy range $U_n$ to $U_{n+1}$. This probability may be written as

$$Q_{n,\,ex}(U_n, E_2) = Q(U_n, E_2) - Q(U_{n+1}, E_2) \quad cm^2 \tag{21}$$

In equation (21) the quantities $U_n$ and $U_{n+1}$, respectively, are substituted for $U$ in equation (17). The choice of the $U_{n+1}$ level is critical in determining the value of the

cross section particularly at high values of $E_2$ where $Q(U_n)$ and $Q(U_{n+1})$ are of comparable value. This fact raises the question of whether the limiting state chosen as $U_{n+1}$ should be either (1) the next spectroscopically allowed state or (2) merely the next electronic state. The most obvious choice for cases of radiation allowed excitation is the first procedure because the chance of an incoming electron exciting an optically forbidden state is considerably less than that of exciting an allowed state.

When cross sections are calculated for forbidden levels, however, two major difficulties arise (1) the choice of the cross section expression to be used and (2) the choice of the $U_{n+1}$ level to be used. In regard to the first case the comparison with the experimental data (see appendix C) suggests certain rules for application of the classical expressions to these excitation processes. The following major rules have therefore been adopted. It appears that satisfactory agreement is obtained with experiment if the Gryzinski exchange cross section is used to describe collisions where $\Delta S \neq 0$; however, the same cross section is unsatisfactory for $\Delta L \neq \pm 1$, $\Delta S = 0$ collisions. Although the exchange peak value is sometimes satisfactory for $\Delta L = \pm 2$, $\Delta S = 0$ collisions there is a large discrepancy in the shapes of the theoretical and experimental excitation functions. The aforementioned results are roughly in agreement with the results of the quantum mechanical predictions of Ochkur (ref. 9) for exchange transitions. In calculating the exchange cross sections for an atom such as helium, there are several choices for the $U_{n+1}$ state. These choices are the following:

(1) The next forbidden state with the same multiplicity as the $U_n$ state

(2) The next forbidden state with different multiplicity

(3) The next forbidden state with the same $L$ value as the $U_n$ state (same multiplicity)

The classical approach to the problem suggests that there are equal probabilities that the final (bound) electron spin will be parallel or antiparallel to the original electron spin after an exchange collision. Then an effective probability factor of $p = 1/2$ can be assumed in the calculated exchange cross section, and the $U_{n+1}$ state will have the same multiplicity as the $U_n$ state. The choice of the $U_{n+1}$ state (for exchange collisions) is therefore resolved into choosing the next state in the same spectral series (same $L$ value as the $U_n$ state) or the next state with the same multiplicity. On the basis of agreement with experimental data, the next state in the same spectral series was used except for the $\Delta L \neq \pm 1$ transitions in cesium where all states have effectively the same multiplicity. A comparison of the calculated semiclassical cross sections with available experimental data is given in appendix C. When the theoretical cross sections are used, the appropriate collision coefficients are obtained from the relation

$$\langle Q_n(v_e)v_e \rangle = \frac{8\pi}{C_o} \int_{U_n}^{\infty} Q_{n,\,ex}(U_n, E_2) \exp\left(\frac{-E_2}{kT_e}\right) E_2 \, dE_2 \qquad cm^3 sec^{-1} \qquad (22)$$

where $Q(U_{n+1}, E_2) = 0$ for $E_2 < U_{n+1}$. The quantity $C_o$ is a normalization factor equal to $(2\pi kT_e)^{3/2}(m_e)^{1/2}$ and the integration limits refer to the excitation process. The upper limit for ionization would be infinity and the lower limit $U_i$.

## ATOMIC MODELS USED IN DETAILED CALCULATIONS

The energy levels used in the helium, argon, and cesium calculation are shown in figures 1, 2, and 3, respectively. In using the Gryzinski equation for the region of highly excited electronic states, the energy difference between excited states is small. Therefore, the cross sections for the remaining levels can be very well approximated as those for one allowed level. In this case $U_n$ is the energy of the lowest state in the grouped level, $U_{n+1}$ is $U_i$, and the energy loss is considered to be the mean energy between $U_n$ and $U_{n+1}$. This is a reasonable approximation in view of the inverse-square dependence of the excitation cross section on the excitation energy and the high density of excited states near the continuum.

For cases when a group of states have essentially the same $U_n$ value, the cross section for the group of levels is calculated using this $U_n$ as the excitation energy. The energy of the next group (next higher principal quantum number) is used as the $U_{n+1}$ value.

## APPROXIMATE THEORY FOR A GENERAL ATOM

Due to the lack of available experimental data, it would be necessary to use theoretically obtained cross sections if these ion production calculations were to be extended to other gases of interest. The detailed atomic structure would have to be considered for each atom and the various individual cross sections would have to be calculated. However, the formulation of the Gryzinski cross sections and the atomic model used in calculating cross sections allow the formulation of an approximate atomic model which yields the ion production results for a general atom. The criterion for the usefulness of this general atom theory will be that its results agree favorably with the more detailed calculations. Favorable comparison of these results with results obtained using experimental helium cross sections would indicate that these semiclassical calculations are reliable for ion production calculations. Agreement with the detailed studies made using the semi-

classical cross sections would indicate that consideration of the discrete atomic structure of the target atom is not necessary.

In the general theory two assumptions are made (1) that the ionization and excitation cross sections are obtained from equations (16) and (17) and (2) that the atomic structure of the atom consists of one allowed excited energy level. The threshold energy of this level is that of the first excited state $U_l$, and its cutoff energy is the ionization potential $U_i$. The energy loss associated with an excitation into this state is chosen to be either the mean energy of the state $(U_l + U_i)/2$ or the threshold energy $U_l$. The results will be obtained for both of these models and compared with those of the more detailed calculations. Using the one-level model results in the following ion production cost:

$$\varphi = \frac{\langle Q_{ex}(U_l)\rangle \bar{U} + \langle Q(U_i)\rangle U_i}{\langle Q(U_i)\rangle} \quad \text{eV/ion} \tag{23}$$

where $\bar{U}$ is the energy loss assigned to the excitation and the brackets again define collision coefficients for excitation and ionization. However, $\langle Q_{ex}(U_l)\rangle$ is given by

$$\langle Q_{ex}(U_l)\rangle = \langle Q(U_l)\rangle - \langle Q(U_i)\rangle \quad \text{cm}^3\text{sec}^{-1} \tag{24}$$

where the brackets are understood to enclose a product of cross section and velocity. Using equations (16) and (17) gives

$$Q(U_l) = \frac{M\sigma_o}{U_l^2}\frac{U_i}{E_2}\left(\frac{E_2}{E_2+U_i}\right)^{3/2}\left[\frac{U_l}{U_i} + \frac{2}{3}\left(1 - \frac{U_l}{2E_2}\right)\ln\left(2.7 + \sqrt{\frac{E_2 - U_l}{U_i}}\right)\right] \times \left(1 - \frac{U_l}{E_2}\right)^{(2U_i+U_l)/(U_i+U_l)} \quad \text{cm}^2 \tag{25}$$

Considering the dimensionless incident electron energy $x = E_2/U_i$ and letting the dimensionless excitation potential be $y = U_l/U_i$ results in

$$Q(U_l) = \frac{M\sigma_o}{U_l^2}\frac{1}{x}\left(\frac{x}{x+1}\right)^{3/2}\left[y + \frac{2}{3}\left(1 - \frac{y}{2x}\right)\ln\left(2.7 + \sqrt{x - y}\right)\right]\left(1 - \frac{y}{x}\right)^{(y+2)/(y+1)} \quad \text{cm}^2 \tag{26}$$

In the case of ionization, $y = 1$ and equation (24) may be rewritten with the use of equation (16) as

$$\langle Q_{ex}(U_l)\rangle = \frac{M\sigma_o}{U_l^2}\langle g_Q(x, y)\rangle - \frac{M\sigma_o}{U_i^2}\langle g_Q(x, 1)\rangle \qquad cm^3 sec^{-1} \tag{27}$$

The expression for $\varphi$ becomes therefore

$$\varphi = \frac{M\sigma_o\left[\frac{\langle g_Q(x, y)\rangle}{U_l^2} - \frac{\langle g_Q(x, 1)\rangle}{U_i^2}\right]\bar{U} + \frac{M\sigma_o}{U_i^2}\langle g_Q(x, 1)\rangle U_i}{\frac{M\sigma_o}{U_i^2}\langle g_Q(x, 1)\rangle} \qquad eV/ion \tag{28}$$

which reduces to

$$\varphi = U_i + \left[\frac{1}{y^2}\frac{\langle g_Q(x, y)\rangle}{\langle g_Q(x, 1)\rangle} - 1\right]\bar{U} \qquad eV/ion \tag{29}$$

Now define the dimensionless volume ion production cost $\varphi'$ such that

$$\varphi' = \frac{\varphi}{U_i} = 1 + \left[\frac{1}{y^2}\frac{\langle g_Q(x, y)\rangle}{\langle g_Q(x, 1)\rangle} - 1\right]\frac{\bar{U}}{U_i} \tag{30}$$

which becomes

$$\varphi' = 1 + \left[\frac{1}{y^2}\frac{\langle g_Q(x, y)\rangle}{\langle g_Q(x, 1)\rangle} - 1\right]\frac{1 + y}{2} \tag{31}$$

or

$$\varphi' = 1 + \left[\frac{1}{y^2}\frac{\langle g_Q(x, y)\rangle}{\langle g_Q(x, 1)\rangle} - 1\right]y \tag{32}$$

if $\bar{U}$ is chosen to be $(U_l + U_i)/2$ or $U_l$, respectively.

# RESULTS AND DISCUSSION

## Monoenergetic Beam Case

The ion production costs for the monoenergetic beam case using the energy levels in figures 1 to 3 are presented as a function of beam energy by the solid curves in figure 4. For the three gases this cost drops very sharply as the beam energy increases from the ionization potential to a few volts above the ionization potential. The costs for the helium and argon atoms are seen to decrease in a slightly irregular manner as the beam energy is further increased. The relative trends of the curves are as would be expected from an inspection of the atomic structure of the atoms involved. The cost is highest for helium (highest first excited state and ionization potential) and lowest for cesium (lowest first excited state and ionization potential). Because of the large number of terms carried in the determination of $\varphi_B$ (eqs. (3) to (7)), the calculations had to be terminated at an energy that would allow a maximum of three ionizations. Consequently, comparison of the costs for the three atoms cannot be made over a wide range of energies. The dotted portion of the cesium curve was obtained by considering only two cross sections, that is, the total excitation cross section with an associated energy loss of 2.66 electron volts and the ionization cross section. This approximation allowed the cesium results to be carried to higher beam energies.

## Results for the Maxwellian Distribution

The results of the Maxwellian electron energy distribution calculations are shown in figure 5 which is a plot of the volume ion production cost against electron kinetic temperature. The ion production cost for each of the atoms is seen to decrease sharply with increasing temperature up to about 12 electron volts. The cost then decreases slowly as the temperature is increased to 40 electron volts. The results of reference 5 are also included in figure 5 to indicate the effect of metastable atoms on the volume ion production cost calculations. As would be expected, the energy cost per ion was the greatest for helium and the least for cesium.

In order to facilitate the use of these results in other calculations such as power balance or species continuity, two additional curves are presented for each of the gases. An ion production rate parameter $\dot{N}_{ion}/N_o N_e$ (eq. (11)) is plotted as a function of electron kinetic temperature in figure 6. Figure 7 shows the variation with electron kinetic temperature of the power consumption rate parameter for inelastic processes $\varphi\dot{N}_{ion}/N_o N_e$ (eq. (15)).

## Discussion of Detailed Cases

The results for the monoenergetic beam are compared with the electron energy distribution results at the average electron kinetic temperature in figure 8. The costs for the distribution case are considerably lower than those for the beam case. This result was expected since the high energy tail of the distribution operates in a region where ionization is more probable than excitation.

The values for the various collision times as calculated in appendix B are shown in figure 9. The plasma conditions assumed are neutral particle density of $10^{12}$ centimeters$^{-3}$, a fraction ionized of 10 percent ($N_e = 10^{11}$ cm$^{-3}$), and an electron temperature varying from 0.5 to 10 electron volts. The electron-electron energy relaxation time and the inelastic electron-neutral collision time are plotted against the monoenergetic electron beam energy in figure 9. The growth time for plasma oscillations has been calculated by considering the two-stream instability analysis in appendix B. For a plasma electron density of $10^{11}$ centimeters$^{-3}$, the growth time would be of the order of $10^{-9}$ seconds which is very much less than the times shown in figure 9. Consequently, an electron beam impinging on the partially ionized plasma would probably have its energy randomized to some energy different from the beam energy and the electron kinetic energy of the plasma. The net energy cost per ion in this case would likely be below that for a monoenergetic beam and approach the electron distribution results at the average electron kinetic temperature shown in figure 8.

## General Theory Results

The results presented for the general study are the ionization cross section, total excitation cross section, Maxwell averaged ionization cross section, and energy cost per ion for a general atom. The quantity $(U_i^2/M)Q^+(U_i)$ is plotted against $x = E_2/U_i$ in figure 10, and the results must be multiplied by $M/U_i^2$ to get the ionization cross section. Figure 11 is the total excitation cross section function as a function of x; in this case, the results must be multiplied by the appropriate $M/U_l^2$ to get the total excitation cross section. Curves for $y = U_l/U_i = 0.3$ to 0.8 are included. The ion production rate parameter $\dot{N}_{ion}/N_o N_e = \langle Q^+(v_e)v_e \rangle \equiv \langle Q(U_i) \rangle$ may be obtained for a general atom from figure 12. Here the results must be multiplied by $M/U_i^{3/2}$ to get the desired quantity. Finally $\varphi'$, the dimensionless volume ion production cost, is plotted against z ($z = kT_e/U_i$) in figures 13 and 14 with y as a parameter. Figure 13 gives the results for the case $\bar{U} = (U_l + U_i)/2$ and figure 14 gives those for $\bar{U} = U_l$. From these figures the volume ion production cost for any atom may be obtained. Cross plots for y values not shown in figures 13 and 14 are given in appendix D.

## Comparison of General and Detailed Calculations

The results obtained from the general atom theory are compared with those for the more detailed study in figure 15. The results of the general atom study agree with the helium results obtained using experimental cross section data to within about 12 percent. This agreement would seem to indicate that the Gryzinski cross sections provide a good approximation for the ion production cost in lieu of available experimental data. The comparisons with the detailed studies made for argon and cesium using the theoretical cross sections show that the results for $\overline{U} = (U_l + U_i)/2$ agree to within about 14 percent for argon and 50 percent for cesium. The $\overline{U} = U_l$ case is seen to give much better agreement in the cesium case. Such agreement should be expected from a study of the arrangement of the atomic energy levels for the various atoms. The levels are distributed such that the best results should be obtained if the $\overline{U} = (U_l + U_i)/2$ case is used when $U_l/U_i > 0.45$ and the $U = U_l$ case when $U_l/U_i < 0.45$. This fact is substantiated by the results shown in figure 15. The former choice corresponds to the rare gas case where the first excitation energy is nearly equal to the ionization energy. The latter case more nearly corresponds to the alkali atoms for which the first excitation energy is about one third the ionization energy. The results presented in figure 15 indicate that reliable ion production cost information can be obtained without considering the discrete atomic structure of the atoms involved.

## CONCLUDING REMARKS

The semiclassical Gryzinski technique has been used to calculate the various cross sections needed to perform the ion production cost calculations in helium, argon, and cesium gases. In general these cross sections are found to agree with existing experimental data to within a factor of two or better. A discussion of this theory, its limitations, and various atomic models to be used in conjunction with this method is presented as well as a detailed comparison with the existing experimental data.

These cross sections were used to determine the ion production results for cesium and argon for the cases of (1) a monoenergetic beam incident upon a cold neutral gas and (2) a thermal electron gas interacting with cold neutrals. The energy cost per ion formed was found to be higher for case (1) than case (2) at a beam energy equal to the electron kinetic temperature. The ion production costs exhibit the expected trends, namely, that the atoms with the higher ionization potential and first excited states have the higher ion production costs and that these costs decrease with increasing electron kinetic temperature.

The monoenergetic beam analysis is applicable only to the case of a beam incident

upon a cold neutral gas. If the beam were incident upon a partially ionized plasma, the results of a collision time comparison show that the beam energy would probably be randomized by setting up plasma oscillations. In this case it is assumed that the energy cost would be less than that for the previous case.

In view of the simplicity of using the Gryzinski expression, an approximate ion production cost calculation was made for a general atom. The favorable agreement obtained between this method and the results for helium using experimental cross sections indicate that the use of the Gryzinski cross section is a very good approximation. The general atom results were also found to give very good agreement with the more detailed calculations in argon and cesium. It is therefore apparent that the general atom results can be used rather than make more detailed calculations for ordinary plasma energy balances. The results of a previous calculation (NASA TN D-3121) showing the effects of electron-metastable atom collisions on the volume ion production results has also been presented. These collisions will cause a maximum reduction of cost in the case of the helium atom; since this effect was of the order of 25 percent in helium, they were not considered in the general theory. The general atom results could be applied to atoms in various ionization stages; however, in this case any important interaction with the electronic excited states would have to be accounted for. The electron energy distribution results were derived for the case of steady-state, optically thin, partially ionized plasmas. These plasmas are assumed to have an elevated electron kinetic temperature and a Maxwellian distribution of free electron energies. Such plasmas are commonly generated in the laboratory in conjunction with plasma acceleration devices. Although the results in general represent only a portion of the power consumption rate or species production rate in an actual experiment, they are quite useful. For example, these results could be used to evaluate the moments of the inelastic collision integral of the Boltzmann equation as was done by Chubb and Seikel (NASA TN D-3250) in the study of a low density Hall current ion accelerator. Furthermore, since the results do not depend upon the experimental configuration, they are general enough to be a useful and applicable aid in determining the overall power balance and species continuity calculations for most low pressure plasma devices.

Lewis Research Center,
National Aeronautics and Space Administration,
Cleveland, Ohio, April 14, 1967,
120-26-03-04-22.

# APPENDIX A

## SYMBOLS

| | |
|---|---|
| $C_o$ | normalization factor, $(2\pi kT_e)^{3/2} m_e^{1/2}$, $(eV^{3/2})(g^{1/2})$ |
| E | energy, eV |
| $\dot{E}_{ion}$ | rate at which energy is expended in ionization process, $eV/(cm^3)(sec)$ |
| $\dot{E}_{j,ex}$ | rate at which energy is expended in excitation processes, $eV/(cm^3)(sec)$ |
| $E_1$ | kinetic energy of bound electron in Gryzinski formula, eV |
| $E_2$ | kinetic energy of incident electron in Gryzinski formula, eV |
| e | electronic charge, $1.602\times10^{-19}$ C |
| G(x') | $\varphi(x') - x' \dfrac{d\varphi(x')}{dx'}$ / $2x'^2$ where $x' = (E_B/kT_e)^{1/2}$ and $\varphi(x') = (2/\pi^{1/2}) \int_0^{x'} e^{-f^2}\, df$ |
| $g_{exch}$ | defined by eq. (20) |
| $g_Q$ | defined by eq. (17) |
| $kT_e$ | electron kinetic temperature, eV |
| L | total angular momentum quantum number for atom |
| M | number of equivalent electrons in outer shell of target atom in Gryzinski formula |
| $m_e$ | electron mass, $9.108\times10^{-28}$ g |
| $m_o$ | mass of neutral atom, g |
| N | number density, $cm^{-3}$ |
| $\dot{N}_{ion}$ | ion production rate, $(cm^{-3})(sec^{-1})$ |
| $\dot{N}_j$ | production rate of excited states, $(cm^{-3})(sec^{-1})$ |
| $P_j$ | normalized probability for inelastic process with energy loss $U_j$ |

| | |
|---|---|
| $P^+$ | total normalized probability for ionization |
| $P_n^+$ | normalized probability for ionizing in $n^{th}$ collision |
| $Q$ | inelastic cross section, $cm^2$ |
| $Q_T$ | total inelastic cross section, $cm^2$ |
| $Q^+$ | ionization cross section, $cm^2$ |
| $Q(U, E_2)$ | inelastic cross section represented as function of $U$ and $E_2$ in Gryzinski formula, $cm^2$ |
| $Q(v_e)$ | inelastic cross section represented as function of electron velocity, $cm^2$ |
| $U$ | energy loss in Gryzinski formula, eV |
| $U_i$ | ionization energy, eV |
| $U_l$ | energy of lowest level above ground state in target atom or first excitation potential, eV |
| $U_n$ | excitation energy in Gryzinski formula, eV |
| $U_{n+1}$ | cutoff energy in Gryzinski formula, eV |
| $\overline{U}$ | energy loss in general atom calculations, eV |
| $v$ | velocity, cm/sec |
| $\dot{W}$ | power consumption rate for volume ion production, $W/cm^3$ |
| $x$ | dimensionless incident electron energy, $E_2/U_i$ |
| $y$ | dimensionless excitation energy, $U_l/U_i$ |
| $z$ | dimensionless electron kinetic temperature, $kT_e/U_i$ |
| $\sigma_o$ | constant in Gryzinski cross section expression, $6.51\times10^{-14}$ $(cm^2)(eV^2)$ |
| $\tau_c$ | electron-neutral collision time, sec |
| $\tau_E$ | beam electron - plasma electron collision time, sec |
| $\tau_g$ | growth time for plasma instabilities, sec |
| $\varphi$ | ion production cost in general atom case, eV/ion |
| $\varphi_B$ | ion production cost for monoenergetic beam, eV/ion |
| $\varphi_T$ | ion production cost for electron distribution case, eV/ion |

$\varphi'$ dimensionless volume ion production cost, $\varphi/U_i$

$\omega_p$ plasma frequency, $sec^{-1}$

Subscripts:

B electron beam

e electron

ex excitation

exch exchange

j, k dummy indices

m mean value

o neutral particle

tot total sum of all inelastic processes

# APPENDIX B

## INTERACTION OF MONOENERGETIC ELECTRON BEAM WITH PARTIALLY IONIZED PLASMA

An electron beam incident upon a partially ionized nonequilibrium plasma may interact in a number of different modes. The electron beam may transfer its energy directly to the plasma neutrals or electrons, or it may also initiate plasma oscillations or instabilities. If the beam interacts with the neutrals, it will ionize them directly, as in the monoenergetic electron beam case discussed in the text. If the electron beam interacts with the plasma electrons (which are assumed to have a Maxwellian distribution of electron energies), it will be thermalized with the free-electron gas. If plasma instabilities are generated, the electron beam energy may initially be randomized at some energy different from the beam energy and the plasma electron energy. A cursory analysis of an electron beam plasma interaction may be carried out simply by comparing (1) the time between electron-neutral collisions $\tau_c$, (2) the energy relaxation time for an electron beam thermal electron gas interaction, and (3) the growth time for plasma instabilities. The time between inelastic electron-neutral collisions is given by the expression

$$\tau_c = \frac{1}{N_o Q_T(v_e) v_e} \tag{B1}$$

The energy relaxation time for electron-electron collisions is taken from Spitzer (ref. 10) and may be written as

$$\tau_E = \frac{v_B^3}{6.44\times10^{18}\, N_e \ln\Lambda\, G\left[\left(\frac{E_B}{kT_e}\right)^{1/2}\right]} \tag{B2}$$

where $v_B$ is the velocity of the beam electrons, $\Lambda = (3/2e^3)(k^3T_e^3/\pi N_e)^{1/2}$ in cgs units, and $G\left[(E_B/kT_e)^{1/2}\right]$ is a function of the ratio of the beam energy to the free-electron energy, as defined in appendix A.

A qualitative analysis of the two-stream instability (ref. 11) indicates that the growth time for plasma oscillations is proportional to the plasma period; therefore,

$$\tau_g \propto \frac{1}{\omega_p} \tag{B3}$$

where $\omega_p$ is the plasma frequency equal to $5.64 \times 10^4 N_e^{1/2}$. Typical energy relaxation and electron-neutral collision times are plotted in figure 9. In general, $\tau_g$ will be much less than either of these times.

# APPENDIX C

# CROSS SECTION COMPARISON

In this appendix cross sections obtained using the Gryzinski technique will be compared with the available experimental data for helium, cesium, and argon. The cross sections are compared for the cases of ionization, allowed excitation, total excitation, and radiation forbidden excitation.

In general the semiclassical expressions are found to give good overall agreement (with a factor of 2 or better) with experiment in the cases of ionization, total excitation, allowed excitation, and spin forbidden excitation. The results are not satisfactory for angular momentum forbidden excitations ($\Delta L \neq \pm 1$) when $\Delta S = 0$ is satisfied.

## Ionization

The theoretical ionization cross section for cesium is compared with the experimental results of Brink (ref. 12) and McFarland and Kinney (ref. 13) in figure 16(a). The experimental maximum has been normalized to peak at the same energy as the theoretical curve (15 to 16 eV) since the experimental data were not obtained for these energies. The results agree to within 15 percent for peak absolute value but the agreement is not too good for energies above about 50 electron volts.

A comparison of the results for argon and helium using the experimental data of Smith (ref. 14) and Golden and Rapp (ref. 15) is made in figures 16(b) and (c). Reference 15 did not employ mass analysis but the $Ar^{++}$ relative contribution has been obtained from the curve shape given by Bleakney (ref. 16). The agreement for helium and argon is considered acceptable throughout the energy range for ionization. The threshold behavior for the helium ionization cross section is shown in figure 17(a). The theoretical behavior goes from $\approx(x - 1)^{3/2}$ for $x \leq 1.04$ to a linear dependence on $x$ for $1.04 \leq 2.0$ (ref. 17). Figure 17(b) shows the threshold behavior obtained for argon is in excellent agreement with the experimental data. The cross section is a strong function of $E_1$ near threshold, but the approximation $E_1 = U_i$ is not critical at higher energies.

## Allowed and Total Excitation Cross Sections

The 6p cesium resonance state excitation cross section and the total excitation cross section are compared with the experimental results of Zapesochny and Shimon

(ref. 18) and Nolan and Emmerich (ref. 19), respectively, in figure 18. The calculated cross sections include the direct excitation term only. The exchange contributions which are only significant near threshold are shown in the insert on figure 18. The $U_{n+1}$ level used in the 6p calculation was the 7p state. The total inelastic cross sections have been calculated by letting $U_n$ be the excitation of energy of the first excited state in the atom $U_l$ and $U_{n+1} = U_i$, the ionization potential of the atom being considered. It can be seen from the figure that both calculated cross sections agree with the experimental data to within a factor of two over most of the energy range shown. The slope of the 6p cross section differs from the experimental data by about a factor of three near threshold ($25\ \text{Å}^2/\text{eV}$ compared with $72\ \text{Å}^2/\text{eV}$). The threshold behavior is important for calculations on low temperature plasma ($kT_e < 1$ eV) (ref. 20) where in the case of cesium all electrons of interest have energies near $U_n$. The sensitivity of the high energy excitation cross sections to the choice of the $U_{n+1}$ level is also illustrated in figure 18 where the curve for the $U_{n+1}$ state is the 5d state as shown (ref. 21). Obviously the choice of the next state in the same spectral series as the $U_{n+1}$ state gives best agreement with experiment for allowed transitions in cesium.

The predictions of the Gryzinski theory for the second and third members of the resonance series in helium (i.e., $3^1P$, $4^1P$ levels) are compared with the cross sections presented in references 3 and 22 in figure 19(a). The semiclassical values again agree to within a factor of approximately two with the results of reference 3, and better agreement is obtained at high energy with the results of reference 22. The theoretical values peak earlier than the experimental results and have larger slopes in the region near threshold.

A comparison of the theoretical total excitation cross section in helium with the sum of the individual cross sections given in reference 3 is shown in figure 19(b). Agreement is surprisingly good over the entire energy range presented (20 to 200 eV), although a detailed comparison at threshold was not made.

## Excitation of Radiation Forbidden States

The prediction of the semiclassical exchange cross section for the 6s → 7s and 6s → 8s, 6s → 5d, 6s → 6d radiation forbidden transitions ($\Delta L = 0$, $\Delta L = 2$) in cesium are shown in figure 20. The results are compared with inferred experimental values (maximum value and energy) and direct experimental results. In figures 20(a) and (b), the $U_{n+1}$ level was chosen to be the next allowed electronic level (7p and 8p, respectively) instead of the next series level. The probability factor was not included since the excited states are effectively spin degenerate, that is, the energy differences between relative orientations of the spin and angular momentum can be neglected. Curves for these exchange cross sections where the $U_{n+1}$ state is chosen to be the next series state

(8s, 9s) were found to give only slightly better agreement with experiment as regards shape. However, their maximum values were generally a factor of two larger than the experimental value. The maximum cross section values for either choice of $U_{n+1}$ values are in reasonable agreement with experiment. However, the calculated cross sections decrease much more rapidly with increasing electron energy than the experimental cross sections. In figures 20(c) and (d) the $U_{n+1}$ values used were the 7s and 8s levels, respectively. The calculated 6s → 5d cross section also has the proper maximum value but decreases too rapidly with increasing electron energy. The calculated 6s → 6d cross section exhibits very poor overall agreement with experiment.

The theoretical curves for the ground state $1^1S \rightarrow 3^1S$ ($\Delta L = 0$) excitation in helium is compared with the results of references 3 and 22 in figure 21(a). As was shown for the alkali case, the theoretical cross section drops off much too rapidly with increasing energy. Virtually identical behavior is observed for the $\Delta L = 2$ ($1^1S \rightarrow 3^1D$) excitation shown in figure 21(b). The $U_{n+1}$ states were chosen to be the next level in the same spectral series although this should not make much difference since the energies of all of the next forbidden levels are about the same.

In helium, comparisons for spin exchange collisions ($\Delta S \neq 0$) may be made. For these collisions the semiclassical exchange cross sections give good agreement with experiment independent of changes in angular momentum quantum number. This can be seen from figures 21(c) and (d) where the results are compared with experiment for excitation from the ground state to the $2^3P$ and $3^3S$ levels, ($\Delta L = 1$ and $\Delta L = 0$, respectively). Again the $U_{n+1}$ states chosen were the next members of the same spectral series. The theoretical cross sections peak at lower energy than the experimental results but exhibit essentially the same shape.

# APPENDIX D

## INTERPOLATION CURVES FOR GENERAL ATOM RESULTS

The results presented for the dimensionless volume ion production cost $\varphi'$ in figures 13 and 14 do not interpolate linearly for y values not presented in these figures. The $\varphi'$ values were therefore normalized to 1 at $y = 0.35$ and plotted against y with the nondimensional electron kinetic temperature ($z = kT_e/U_i$) as a parameter in figures 22(a) and (b). The results in figure 22(a) are for the $\overline{U} = (U_l + U_i)/2$ case, and those in figure 22(b) are for the $\overline{U} = U_l$ case. Table I(a) includes the values of $\varphi'$ and $\varphi'/\varphi'$(at $y = 0.35$) for various y and z values for the $\overline{U} = (U_l + U_i)/2$ case, while table I(b) includes the same results for the $\overline{U} = U_l$ case.

## REFERENCES


1. Chubb, Donald L.; and Seikel, George R.: Basic Studies of a Low Density Hall Current Ion Accelerator. NASA TN D-3250, 1966.

2. Gryzinski, Michal: Classical Theory of Electronic and Ionic Inelastic Collisions. Phys. Rev., vol. 115, no. 2, July 15, 1959, pp. 374-383.

3. Sovie, Ronald J.; and Klein, Barry M.: Volume Ion Production in a Tenuous Helium Plasma. NASA TN D-2324, 1964.

4. Wilson, R.: The Spectroscopy of Non-Thermal Plasmas. J. Quant. Spectr. and Radiative Transfer, vol. 2, 1962, pp. 477-490.

5. Sovie, Ronald J.; and Dugan, John V., Jr.: Effects of Metastable Atoms on Volume Ion Production in a Tenuous Helium Plasma. NASA TN D-3121, 1965.

6. Gryzinski, Michal: Classical Theory of Atomic Collisions. I. Theory of Inelastic Collisions. Phys. Rev., vol. 138, no. 2A, Apr. 19, 1965, pp. 336-358.

7. Prasad, S. S.; and Prasad, K.: Classical Calculations for Impact Ionization Cross Sections. Phys. Soc. Proc., vol. 82, pt. 5, Nov. 1963, pp. 655-658.

8. Vriens, L.: Calculation of Absolute Ionization Cross Sections of He, $He^*$, $He^+$, Ne, $Ne^*$, $Ne^+$, Ar, $Ar^*$, Hg and $Hg^*$. Phys. Letters, vol. 8, no. 4, Feb. 15, 1964, pp. 260-261.

9. Ochkur, V. I.: The Born-Oppenheimer Method in the Theory of Atomic Collisions. Soviet Physics - JETP, vol. 18, no. 2, Feb. 1964, pp. 503-508.

10. Spitzer, L.: Physics of Fully Ionized Gases. Interscience Publ., 1956.

11. Stix, Thomas H.: The Theory of Plasma Waves. McGraw-Hill Book Co., Inc., 1962.

12. Brink, G. O.: Absolute Ionization Cross Sections of the Alkali Metals. Phys. Rev., vol. 134, no. 2A, Apr. 20, 1964, pp. 345-346.

13. McFarland, Robert H.; and Kinney, John D.: Absolute Cross Sections of Lithium and Other Alkali Metal Atoms for Ionization by Electrons. Phys. Rev., vol. 137, no. 4A, Feb. 15, 1965, pp. 1058-1061.

14. Smith, Philip T.: The Ionization of Helium, Neon, and Argon by Electron Impact. Phys. Rev., vol. 36, Oct. 15, 1930, pp. 1293-1302.

15. Englander-Golden, Paula; and Rapp, Donald: Total Cross Sections for Ionization of Atoms and Molecules by Electron Impact. Rep. No. 6-74-64-12, Lockheed Missiles and Space Co., 1964.

16. Bleakney, Walker: Ionization Potentials and Probabilities for the Formation of Multiply Charged Ions in Helium, Neon and Argon. Phys. Rev., vol. 36, Oct. 15, 1930, pp. 1303-1308.

17. Bauer, Ernest; and Bartky, Charlotte D.: Calculation of Inelastic Electron-Molecule Collision Cross Sections by Classical Methods. J. Chem. Phys., 43, no. 7, Oct. 1, 1965, pp. 2466-2476.

18. Zapesochny, I. P.; and Shimon, L. L.: Absolute Excitation Cross Sections of the Alkali Metals. IVth International Conference on the Physics of Electronic and Atomic Collision, Quebec, Aug. 2-6, 1965. Science Bookcrafters, Hastings-on-Hudson, N. Y., 1965, pp. 401-404.

19. Nolan, J. F.; and Emmerich, N. S.: Electron Collision Cross Sections in Metal Vapors. Rep. No. 65-1E5-MHDIN-R1 (NASA CR-54474), Westinghouse Electric Co., Aug. 19, 1965.

20. Dugan, John V., Jr.: Calculation of Three-Body Collisional Recombination Coefficients for Cesium and Argon Atomic Ions with an Assessment of the Gryzinski Cross Sections. J. Appl. Phys., vol. 37, no. 13, Dec. 1966, pp. 5011-5012.

21. Sheldon, John W.; and Dugan, John V., Jr.: Semiclassical Calculations of Inelastic Cross Sections for Electron-Cesium Atomic Collisions. J. Appl. Phys., vol. 36, no. 2, Feb. 1965, pp. 650-651.

22. St. John, Robert M.; Miller, Frank L.; and Lin, Chun C.: Absolute Electron Excitation Cross Sections of Helium. Phys. Rev., vol. 134, no. 4A, May 18, 1964, pp. 888-897.

TABLE I. - DIMENSIONLESS VOLUME ION PRODUCTION COST VALUES AND NORMALIZED DIMENSIONLESS VOLUME ION PRODUCTION COST VALUES FOR VALUES OF DIMENSIONLESS FIRST EXCITATION POTENTIAL $y = U_l/U_i$ AND DIMENSIONLESS ELECTRON KINETIC TEMPERATURE $z = kT_e/U_i$

(a) $\overline{U} = (U_l + U_i)/2$ case.

| Dimensionless electron kinetic temperature, z | Dimensionless first excitation potential, y | | | | | | | | | | | | | | | |
|---|---|---|---|---|---|---|---|---|---|---|---|---|---|---|---|---|
| | 0.35 | 0.40 | 0.45 | 0.50 | 0.55 | 0.60 | 0.70 | 0.80 | 0.35 | 0.40 | 0.45 | 0.50 | 0.55 | 0.60 | 0.70 | 0.80 |
| | Dimensionless volume ion production cost, $\varphi'$ | | | | | | | | Normalized dimensionless volume ion production cost, $\varphi'/\varphi'$ (at y = 0.35) | | | | | | | |
| .1 | 2879 | 1395 | 700 | 361.2 | 190.4 | 102.2 | 30.66 | 9.6 | 1 | 0.481 | 0.242 | 0.125 | 0.0657 | 0.0353 | 0.0106 | 0.0033 |
| .2 | 121.3 | 75.2 | 48.3 | 31.83 | 21.4 | 14.71 | 7.22 | 3.68 | | .62 | .398 | .262 | .176 | .121 | .059 | .03 |
| .3 | 42.26 | 28.53 | 19.9 | 14.28 | 10.45 | 7.79 | 4.50 | 2.69 | | .673 | .47 | .337 | .247 | .184 | .106 | .063 |
| .4 | 24.9 | 17.56 | 12.8 | 9.58 | 7.31 | 5.68 | 3.55 | 2.3 | | .704 | .513 | .384 | .293 | .228 | .142 | .092 |
| .5 | 18.1 | 13.1 | 9.81 | 7.54 | 5.9 | 4.7 | 3.09 | 2.1 | | .723 | .536 | .416 | .326 | .259 | .171 | .116 |
| .6 | 14.6 | 10.77 | 8.21 | 6.42 | 5.12 | 4.14 | 2.81 | 1.97 | | .737 | .562 | .439 | .350 | .283 | .192 | .135 |
| .7 | 12.51 | 9.36 | 7.23 | 5.72 | 4.62 | 3.78 | 2.63 | 1.88 | | .745 | .578 | .457 | .369 | .302 | .210 | .150 |
| .8 | 11.13 | 8.41 | 6.56 | 5.25 | 4.28 | 3.53 | 2.5 | 1.82 | | .755 | .589 | .471 | .384 | .317 | .224 | .163 |
| .9 | 10.16 | 7.74 | 6.08 | 4.9 | 4.02 | 3.35 | 2.4 | 1.77 | | .762 | .598 | .482 | .396 | .33 | .236 | .174 |
| 1.0 | 9.43 | 7.23 | 5.73 | 4.64 | 3.83 | 3.21 | 2.33 | 1.74 | | .766 | .607 | .492 | .406 | .34 | .247 | .184 |
| 1.5 | 7.52 | 5.89 | 4.75 | 3.93 | 3.3 | 2.81 | 2.10 | 1.63 | | .783 | .631 | .52 | .439 | .373 | .279 | .217 |
| 2 | 6.68 | 5.29 | 4.32 | 3.6 | 3.06 | 2.63 | 2.0 | 1.57 | | .792 | .647 | .539 | .458 | .394 | .299 | .235 |
| 2.5 | 6.21 | 4.95 | 4.07 | 3.41 | 2.91 | 2.52 | 1.94 | 1.54 | | .797 | .655 | .549 | .469 | .406 | .312 | .248 |
| 3 | 5.91 | 4.73 | 3.9 | 3.29 | 2.82 | 2.45 | 1.90 | 1.52 | | .799 | .659 | .556 | .477 | .414 | .321 | .257 |
| 4 | 5.54 | 4.47 | 3.70 | 3.14 | 2.70 | 2.36 | 1.85 | 1.49 | | .807 | .668 | .567 | .487 | .426 | .334 | .269 |
| 5 | 5.32 | 4.31 | 3.58 | 3.05 | 2.63 | 2.31 | 1.82 | 1.47 | | .810 | .673 | .573 | .494 | .434 | .342 | .276 |
| 6 | 5.18 | 4.2 | 3.51 | 2.99 | 2.59 | 2.27 | 1.8 | 1.46 | | .8106 | .677 | .577 | .5 | .438 | .347 | .282 |
| 7 | 5.08 | 4.13 | 3.45 | 2.94 | 2.55 | 2.25 | 1.78 | 1.45 | | .813 | .679 | .579 | .502 | .443 | .350 | .285 |
| 8 | 5 | 4.07 | 3.4 | 2.91 | 2.53 | 2.22 | 1.77 | 1.45 | | .814 | .68 | .582 | .506 | .444 | .354 | .290 |
| 9 | 4.94 | 4.03 | 3.37 | 2.89 | 2.51 | 2.21 | 1.76 | 1.44 | | .814 | .681 | .584 | .507 | .446 | .356 | .291 |
| 10 | 4.9 | 3.99 | 3.35 | 2.87 | 2.49 | 2.20 | 1.76 | 1.44 | | .814 | .683 | .585 | .508 | .449 | .359 | .294 |

TABLE I. - Concluded. DIMENSIONLESS VOLUME ION PRODUCTION COST VALUES AND NORMALIZED DIMENSIONLESS VOLUME ION PRODUCTION COST VALUES FOR VALUES OF DIMENSIONLESS FIRST EXCITATION POTENTIAL $y = U_l/U_i$ AND DIMENSIONLESS ELECTRON KINETIC TEMPERATURE $z = kT_e/U_i$

(b) $\overline{U} = U_l$ case.

| Dimensionless electron kinetic temperature, z | Dimensionless first excitation potential, y | | | | | |
|---|---|---|---|---|---|---|
| | 0.35 | 0.40 | 0.45 | 0.35 | 0.40 | 0.45 |
| | Dimensionless volume ion production cost, $\varphi'$ | | | Normalized dimensionless volume ion production cost, $\varphi'/\varphi'$ (at y = 0.35) | | |
| .1 | 1493.6 | 797.7 | 435 | 1 | 0.534 | 0.291 |
| .2 | 63.39 | 43.4 | 30.34 | ↓ | .685 | .479 |
| .3 | 22.4 | 16.73 | 12.74 | ↓ | .747 | .569 |
| .5 | 9.86 | 7.92 | 6.47 | ↓ | .803 | .656 |
| 1 | 5.37 | 4.56 | 3.93 | ↓ | .849 | .732 |
| 2 | 3.95 | 3.45 | 3.06 | ↓ | .873 | .775 |
| 5 | 3.24 | 2.89 | 2.60 | ↓ | .892 | .802 |
| 10 | 3.02 | 2.71 | 2.46 | ↓ | .897 | .815 |

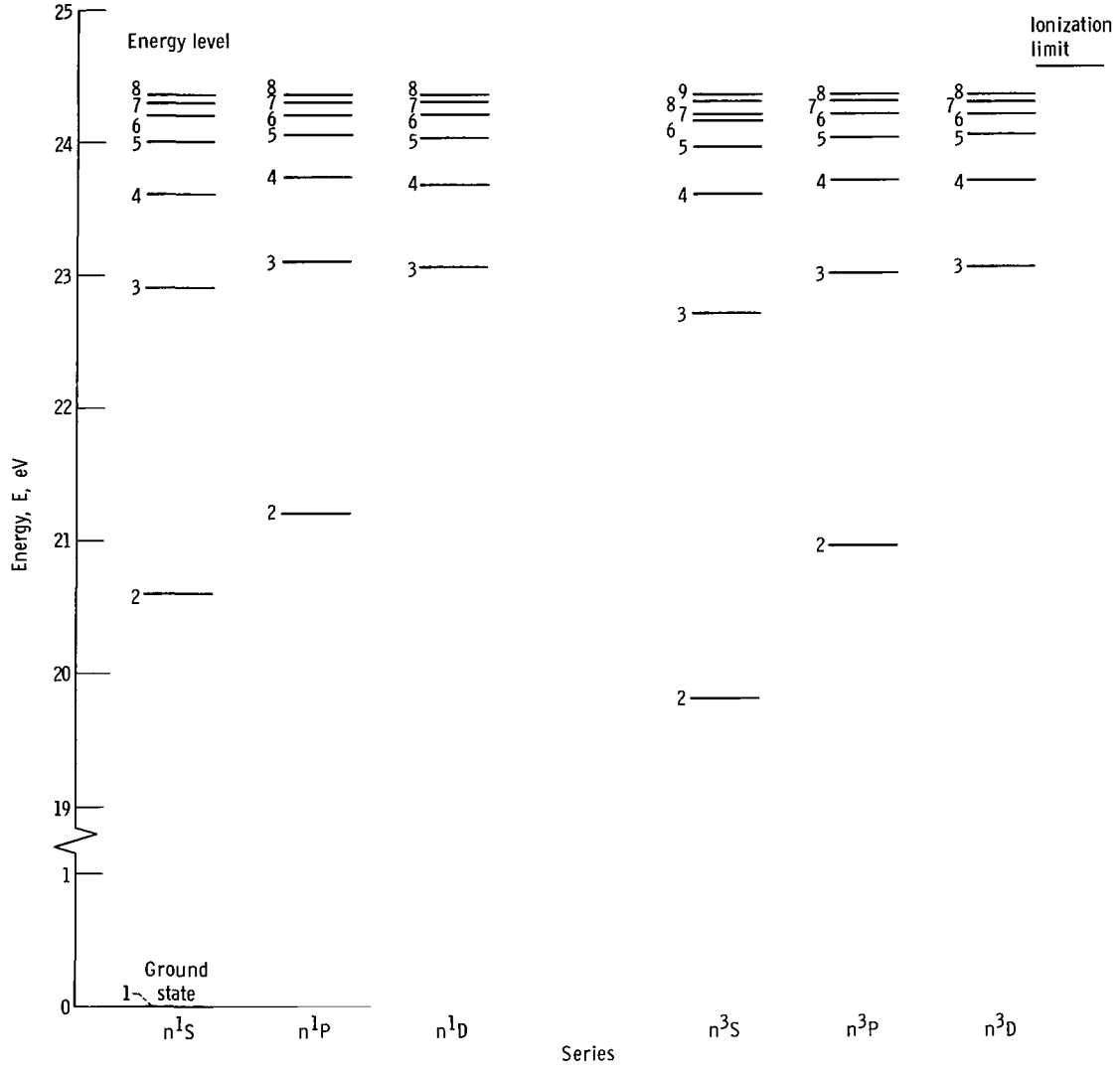


Figure 1. - Energy levels used in detailed helium calculations.

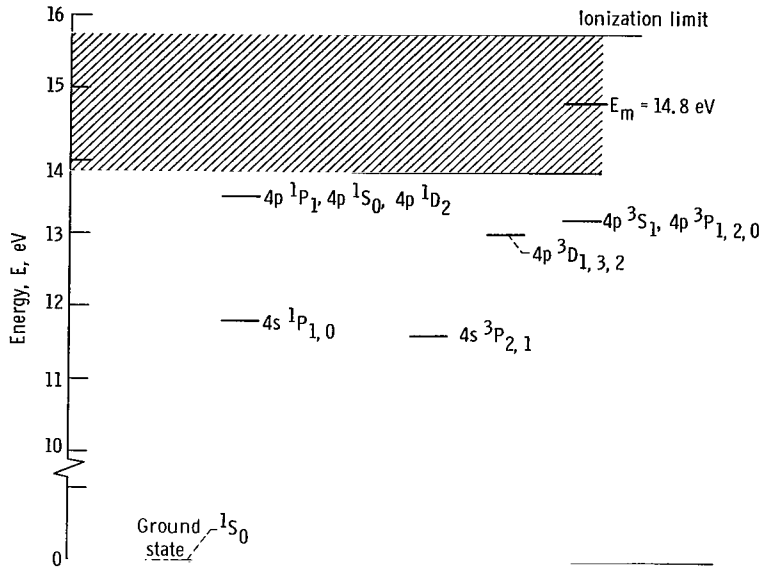


Figure 2. - Energy levels used in detailed argon calculations.

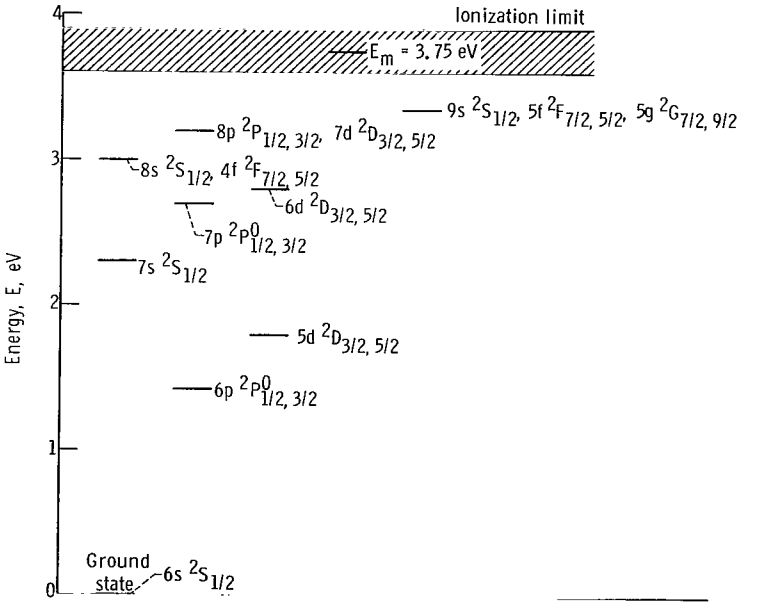


Figure 3. - Energy levels used in detailed cesium calculations.

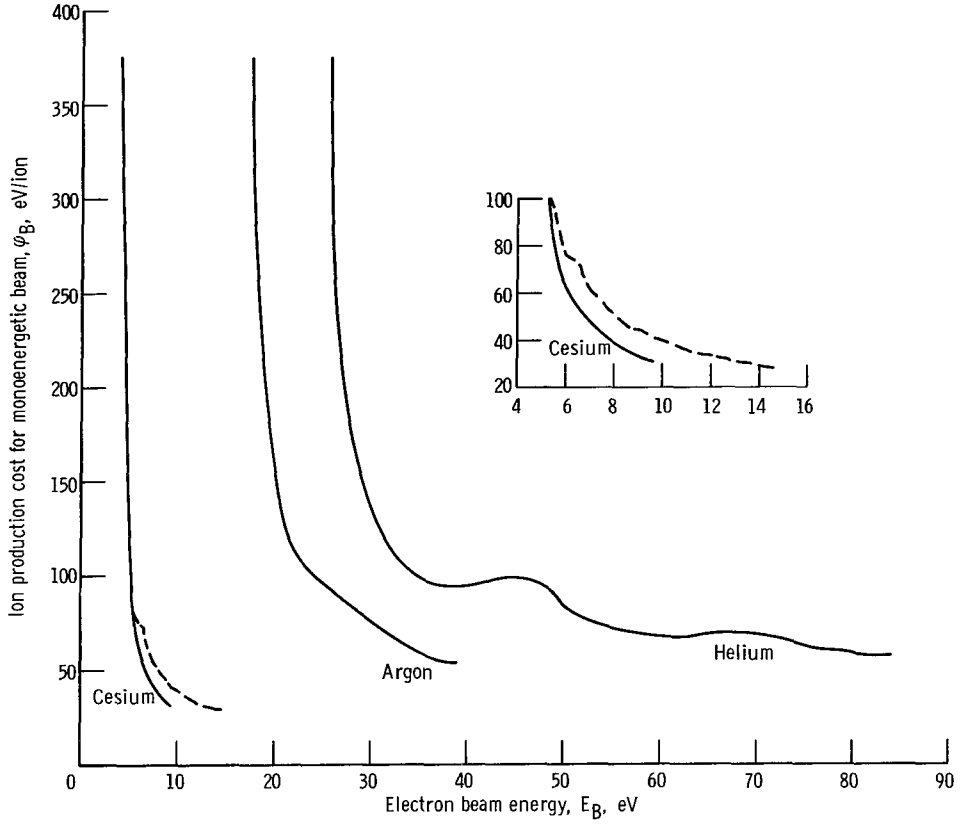


Figure 4. - Ion production cost for monoenergetic beam case as function of electron beam energy.

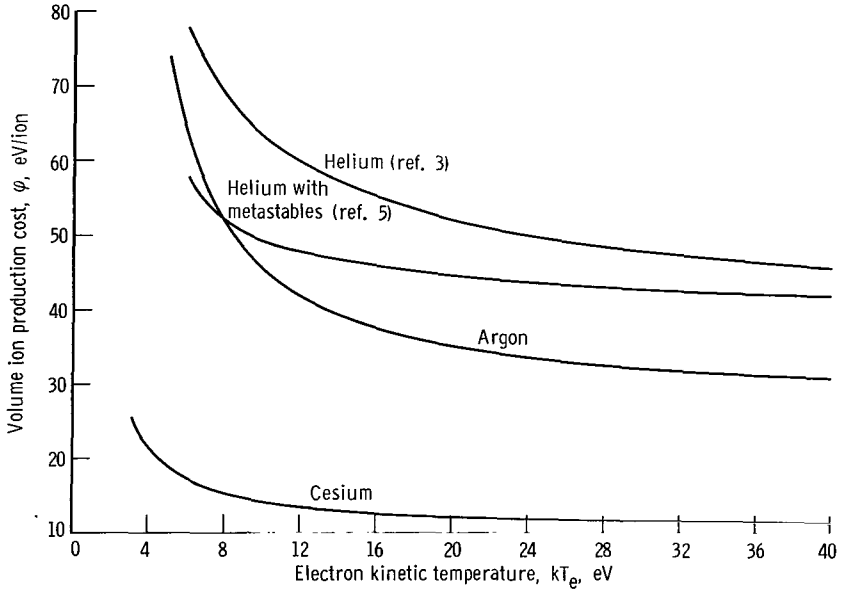


Figure 5. - Volume ion production cost results for detailed calculations as function of electron kinetic temperatures.

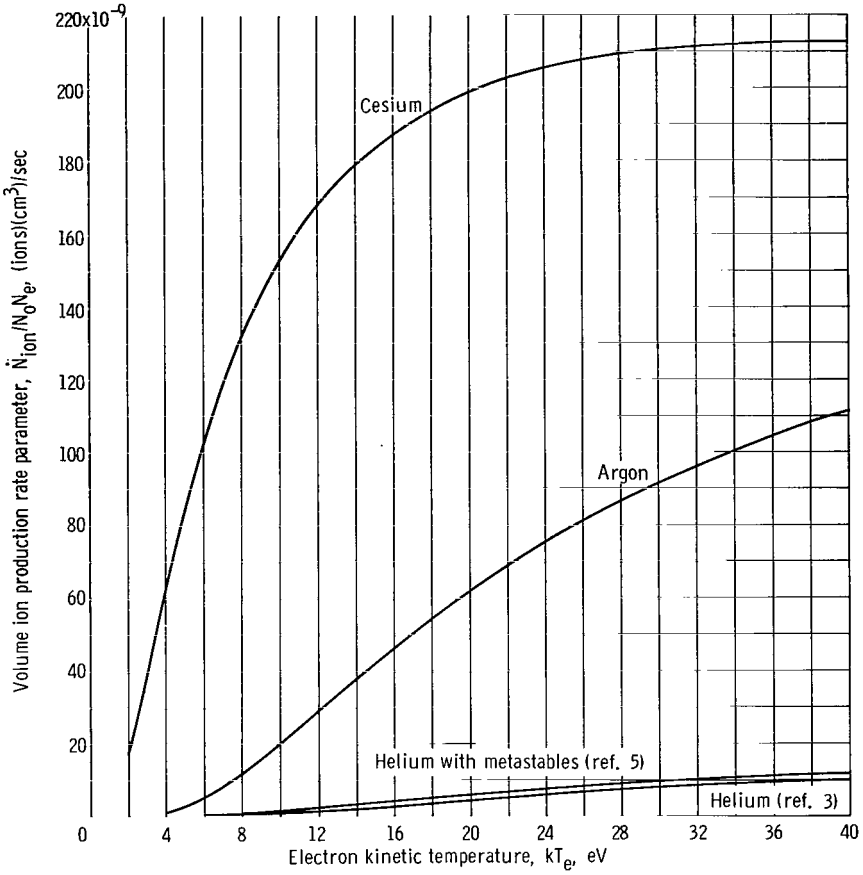


Figure 6. - Volume ion production rate parameter for detailed calculations.

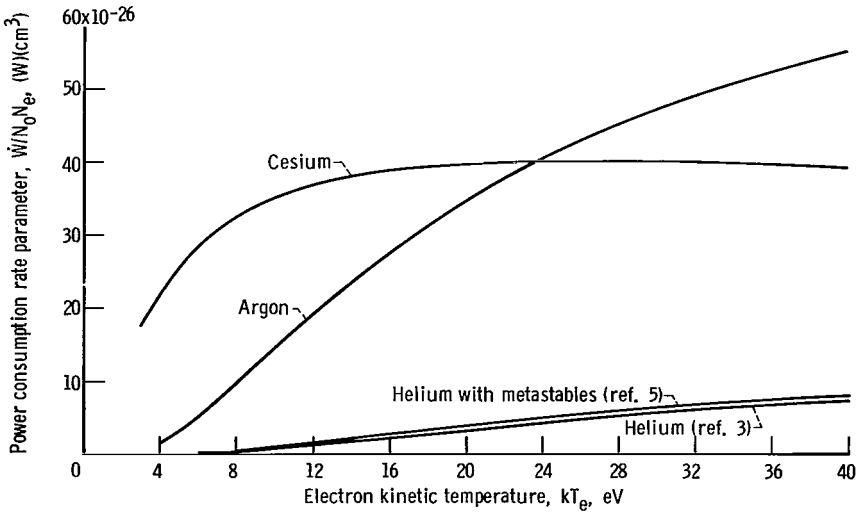


Figure 7. - Power consumption rate parameter from detailed calculations as function of electron kinetic temperature.

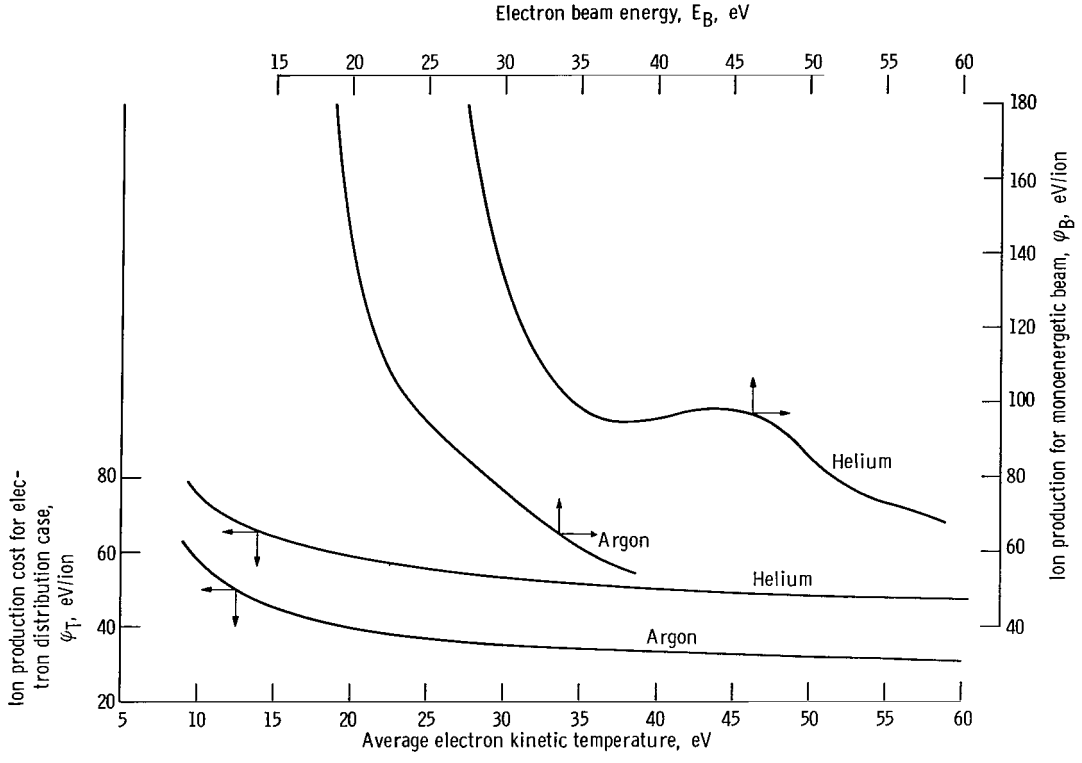


Figure 8. - Comparison of detailed monoenergetic and thermal ion production cost results as functions of average electron kinetic temperature.

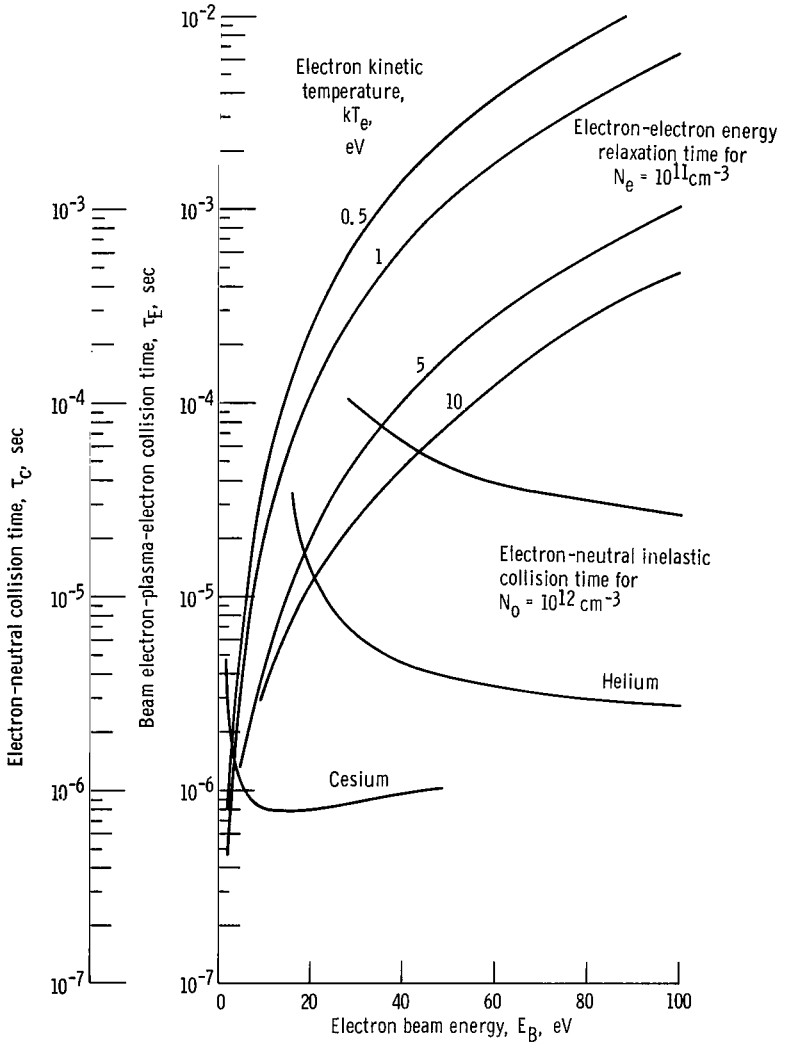


Figure 9. - Collision time comparison for beam electron-plasma-electron and beam electron-plasma-neutral collisions as function of monoenergetic beam energy with plasma electron kinetic temperature $kT_e$ as parameter.

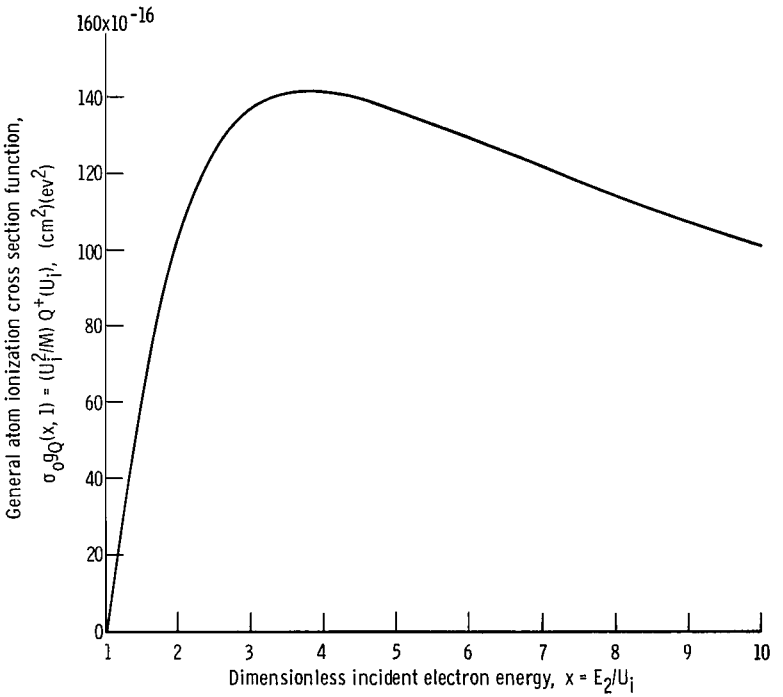


Figure 10. - General atom ionization cross section function plotted against dimensionless incident electron energy $x = E_2/U_i$.

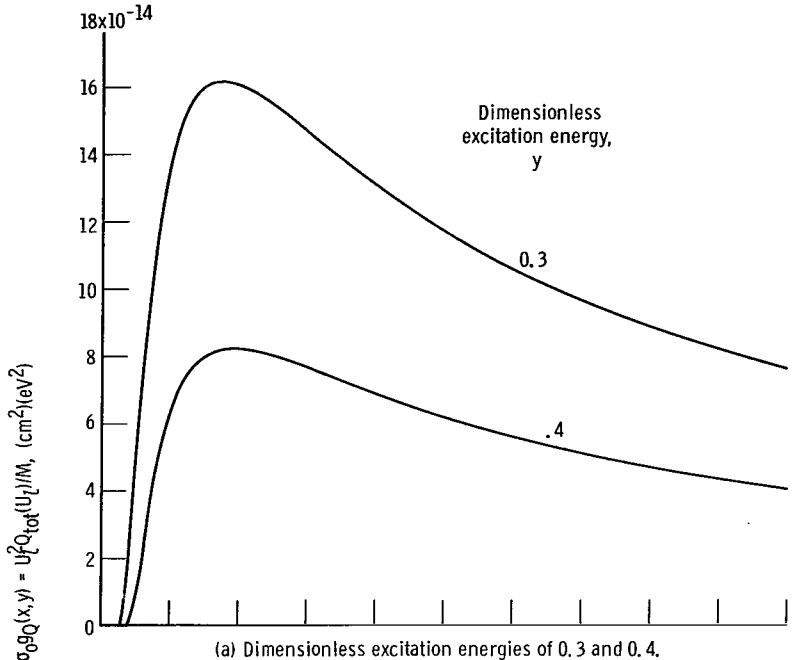


(a) Dimensionless excitation energies of 0.3 and 0.4.

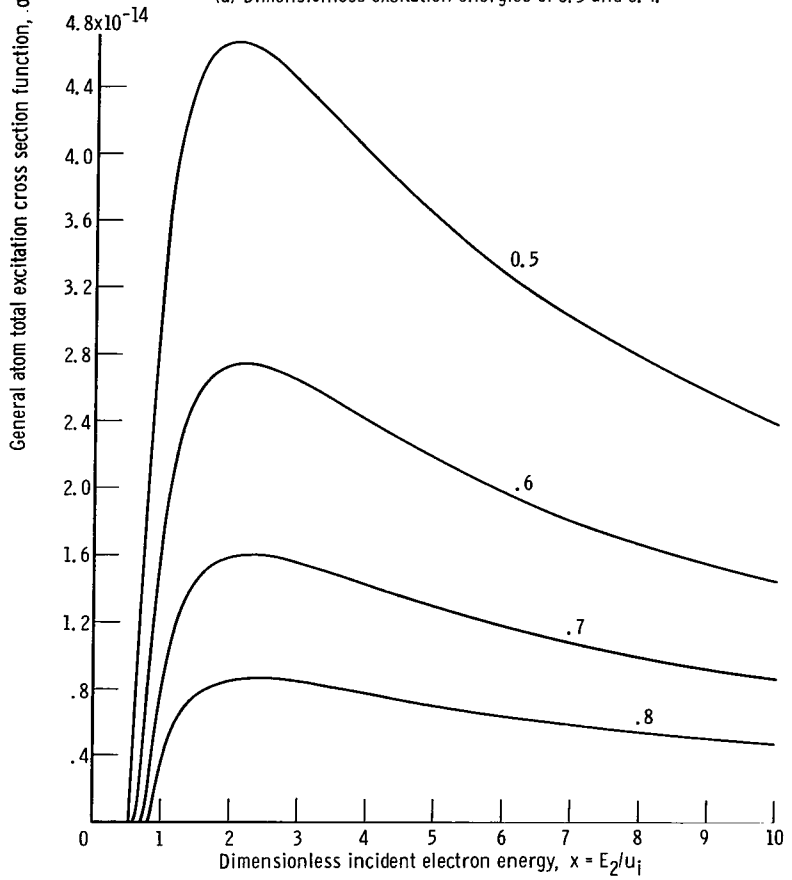


General atom total excitation cross section function, $\sigma_0 g_Q(x,y) = U_i^2 Q_{tot}(U_i)/M$, $(cm^2)/(eV^2)$

(b) Dimensionless excitation energies of 0.5, 0.6, 0.7, and 0.8.

Figure 11. - General atom total excitation cross section function plotted against dimensionless incident electron energy $x = E_2/U_i$

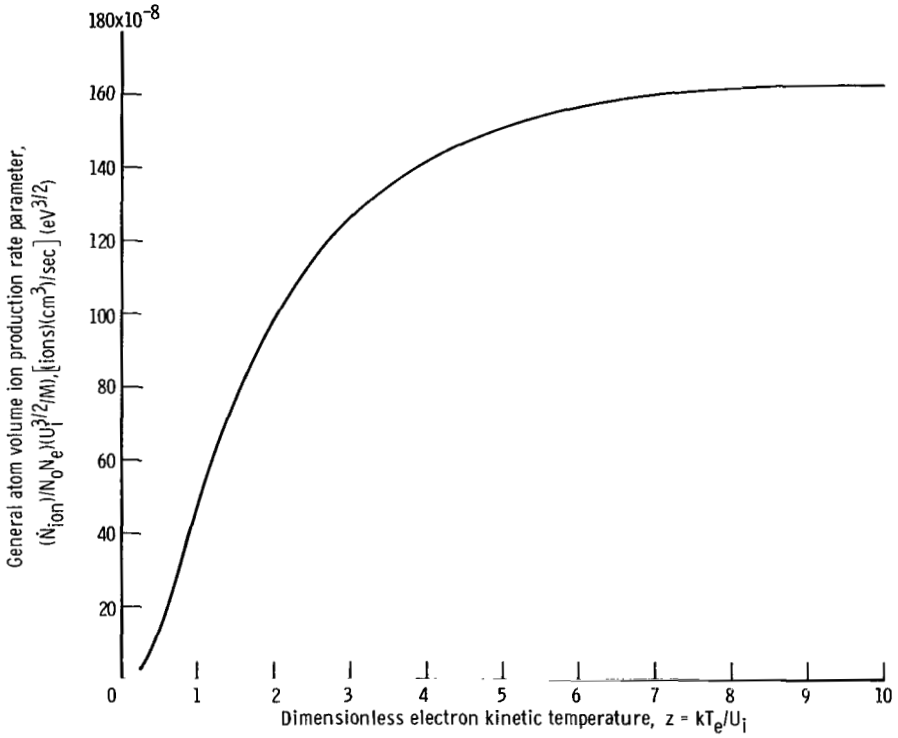


Figure 12. - General atom volume ion production rate parameter plotted against dimensionless electron kinetic temperature $z = kT_e/U_i$.

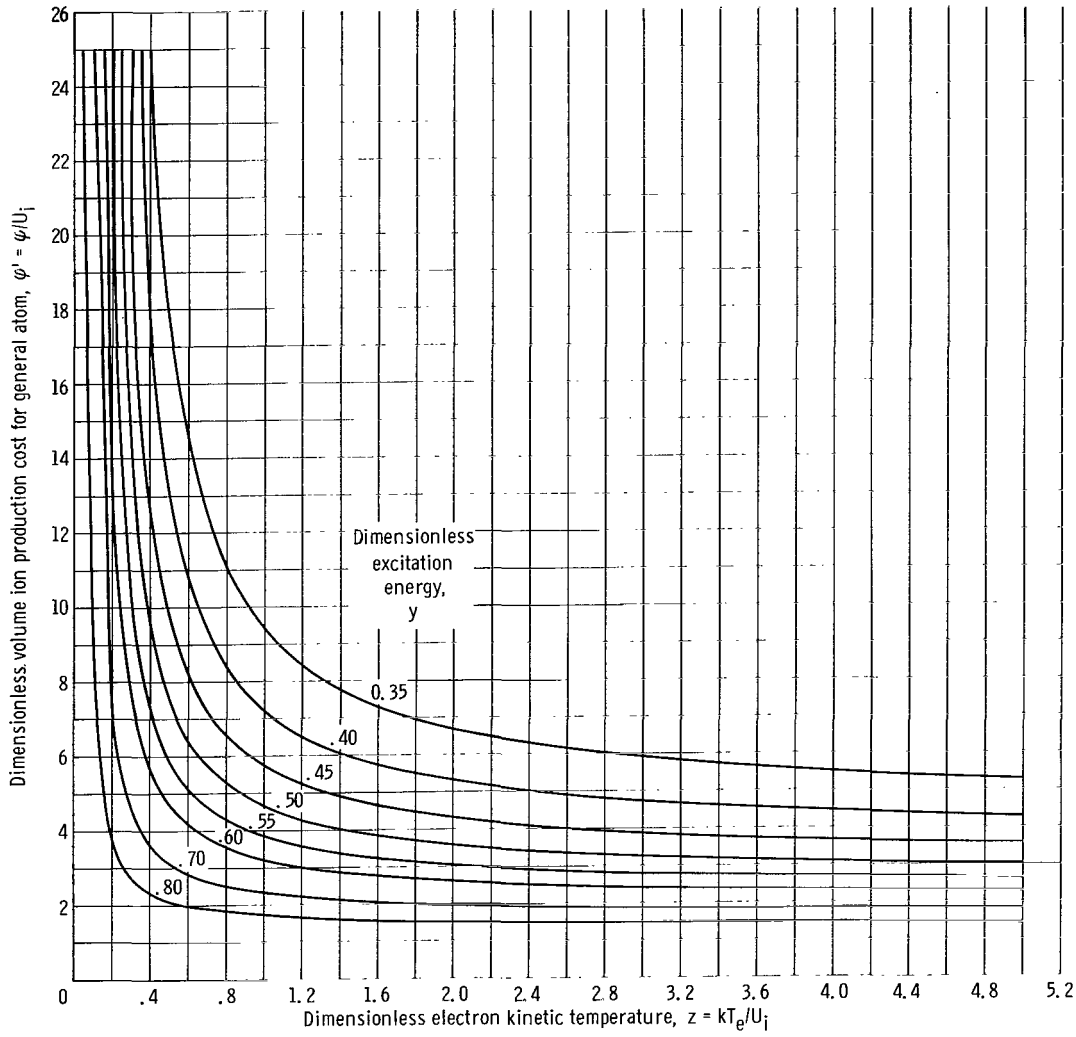


Figure 13. - Dimensionless volume ion production cost for general atom $\varphi' = \varphi/U_i$ plotted against dimensionless electron kinetic temperature $z = kT_e/U_i$ with dimensionless first excitation potential $Y = U_l/U_i$ as parameter $\overline{U} = (U_l + U_i)/2$ case.

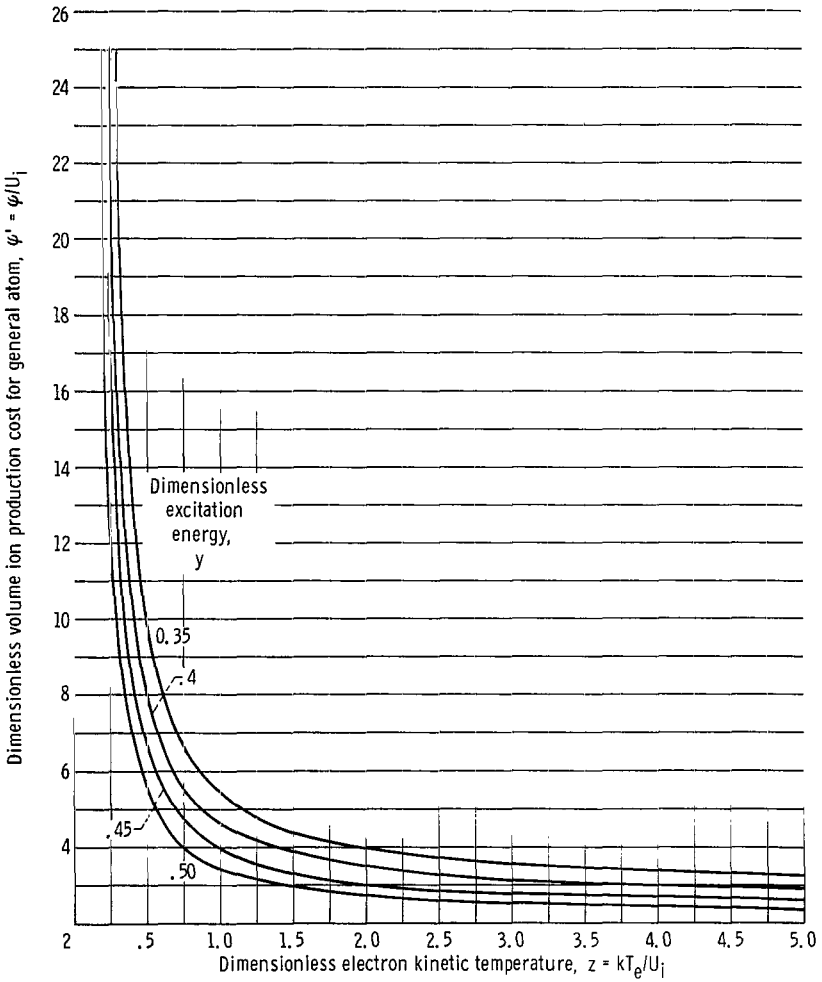


Figure 14. - Dimensionless volume ion production cost for general atom $\varphi' = \varphi/U_i$ plotted against dimensionless electron kinetic temperature $z = kT_e/U_i$ with dimensionless first excitation potential $y = U_l/U_i$ as parameter for $\bar{U} = U_l$ case.

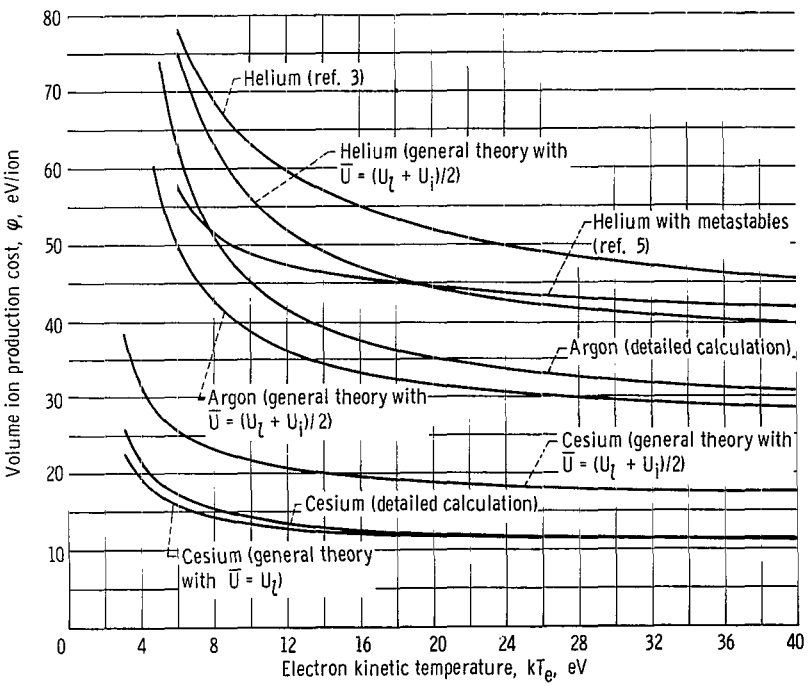


Figure 15. - Comparison of results of general atom theory and detailed calculation for volume ion production cost as functions of electron kinetic temperature.

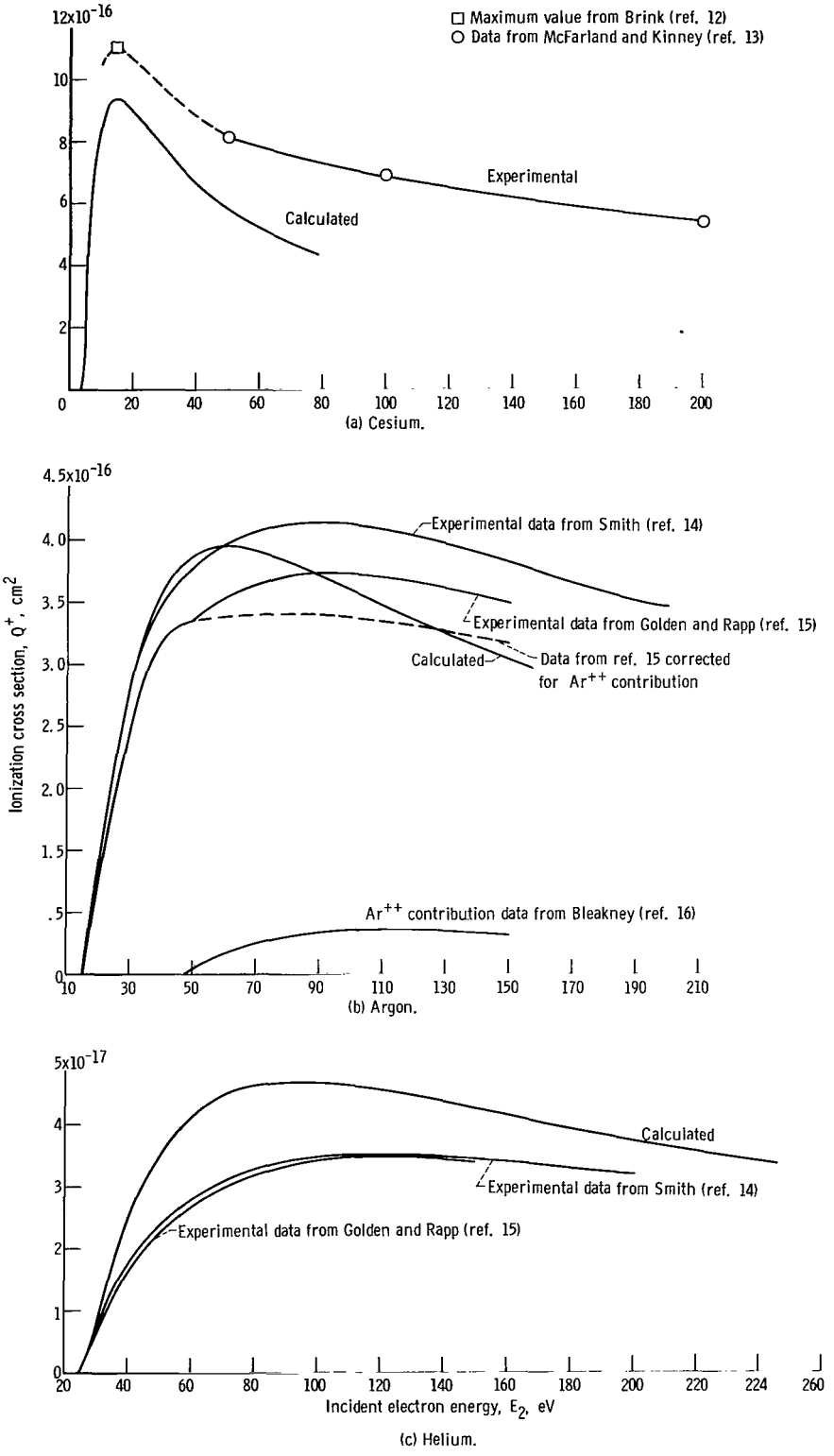


Figure 16. - Comparison of calculated and experimental ionization cross sections as functions of incident electron energy.

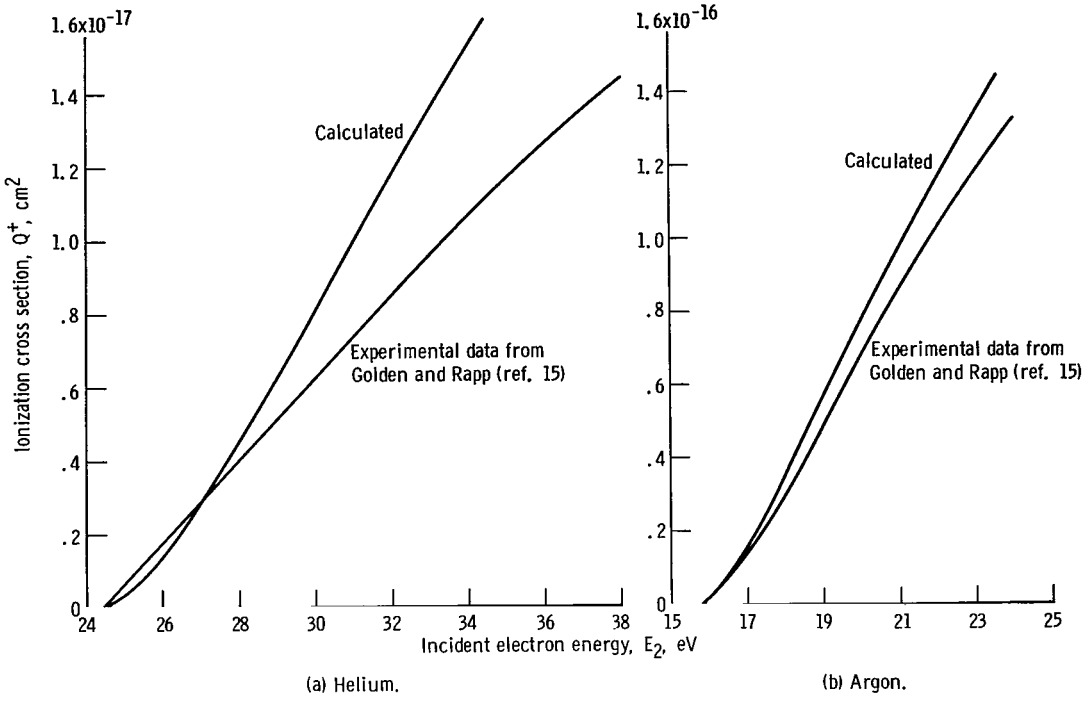


Figure 17. - Comparison of calculated and experimental ionization cross section threshold behavior.

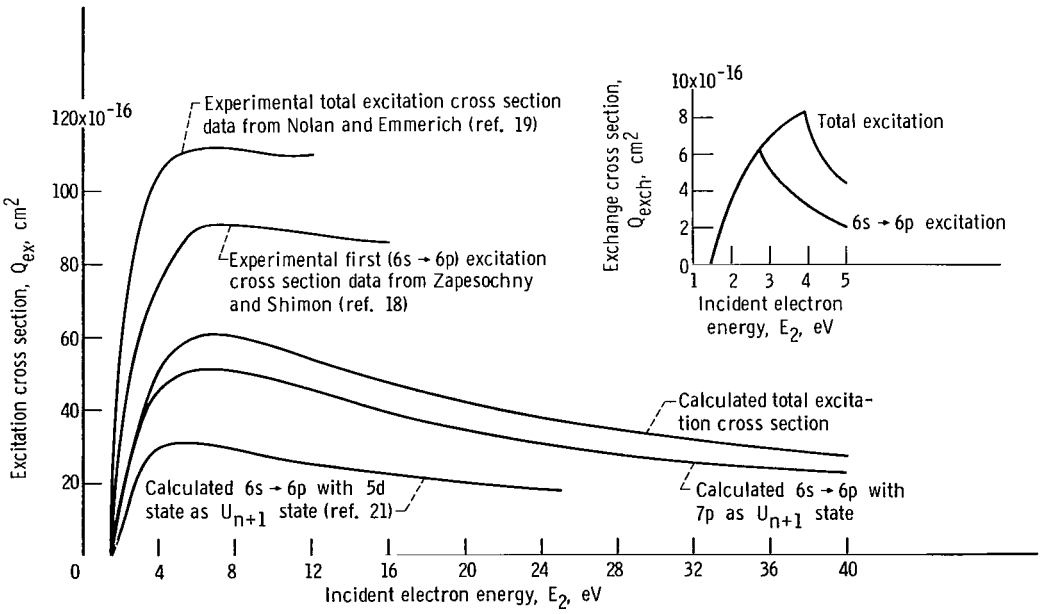


Figure 18. - Comparison of calculated and experimental values for first (6s → 6p) and total excitation cross section in cesium as functions of incident electron energy. Insert is calculated exchange contributions to first (6s → 6p) and total excitation cross sections.

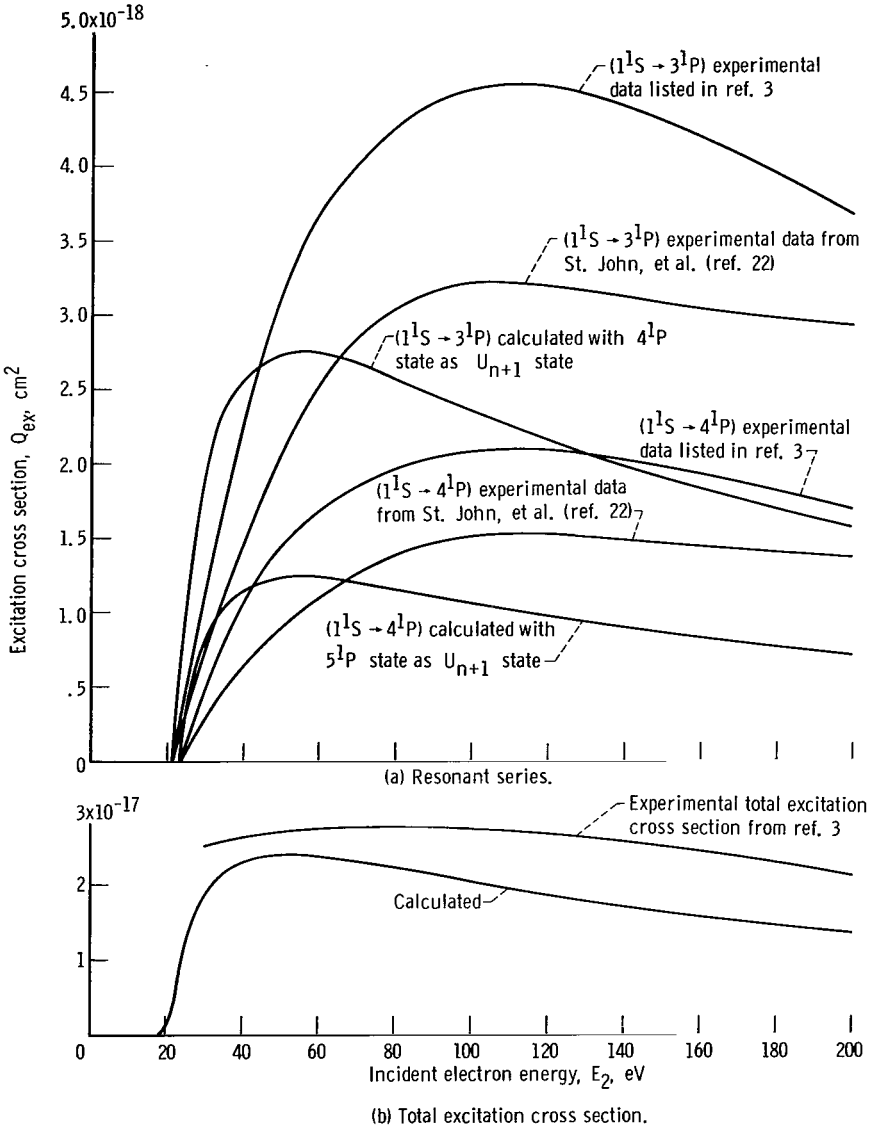


Figure 19. - Comparison of calculated and experimental results for resonant series ($1^1S \rightarrow n^1P$) and total excitation cross sections in helium as functions of incident electron energy.

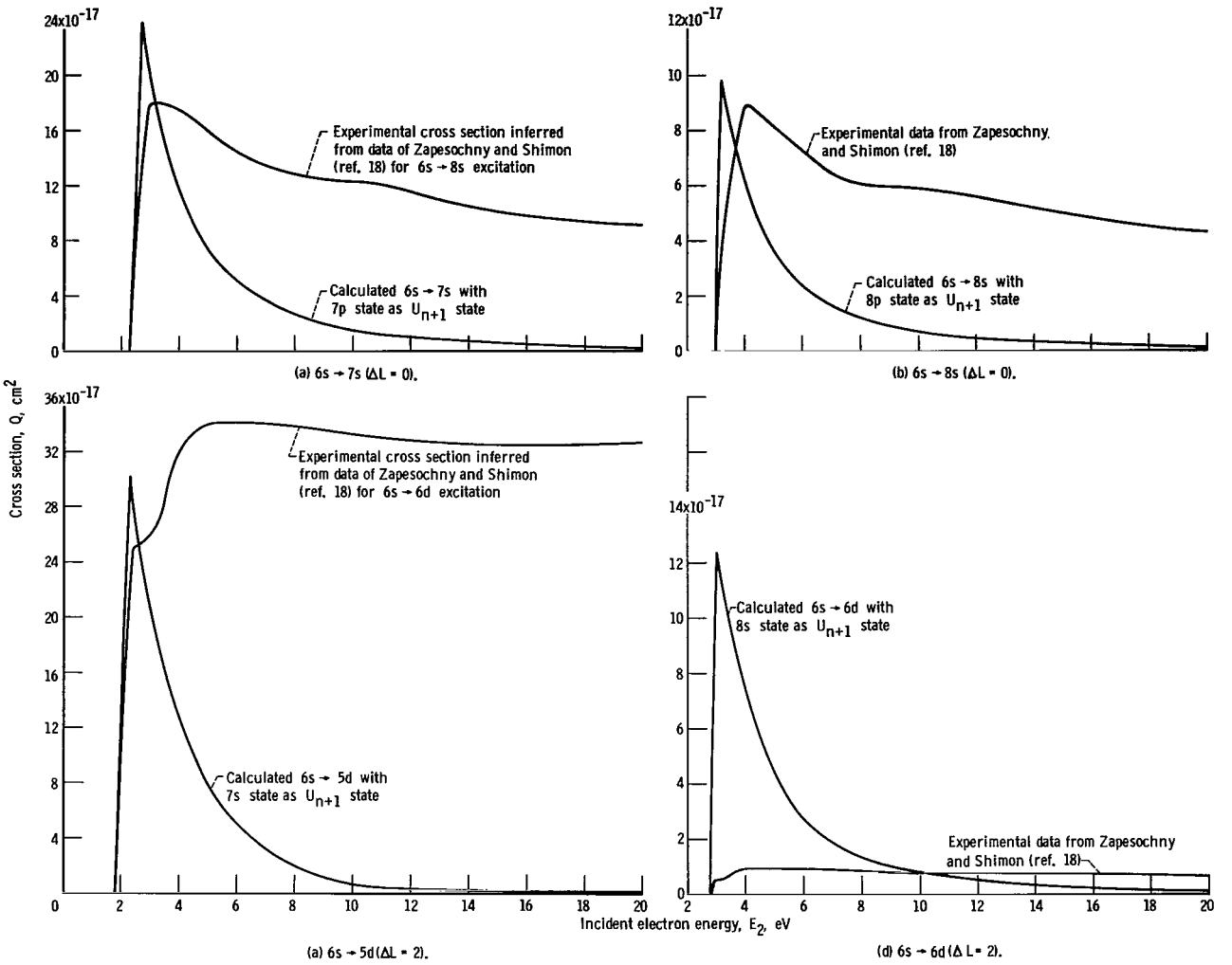


Figure 20. - Comparison of exchange calculations and experimental results for radiation forbidden excitations in cesium as functions of incident electron energy.

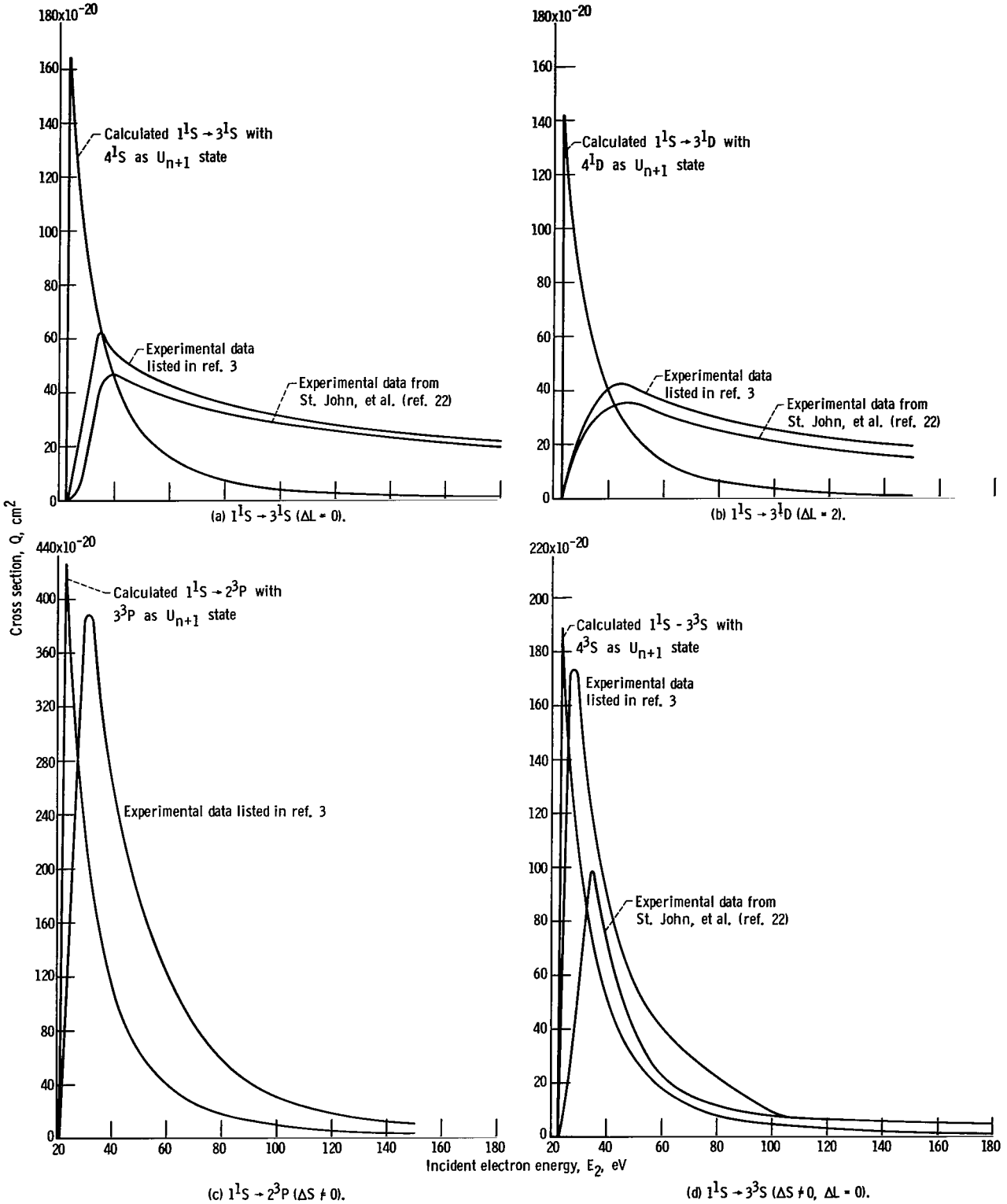


Figure 21. - Comparison of exchange calculations and experimental results for radiation forbidden excitations in helium as functions of incident electron energy.

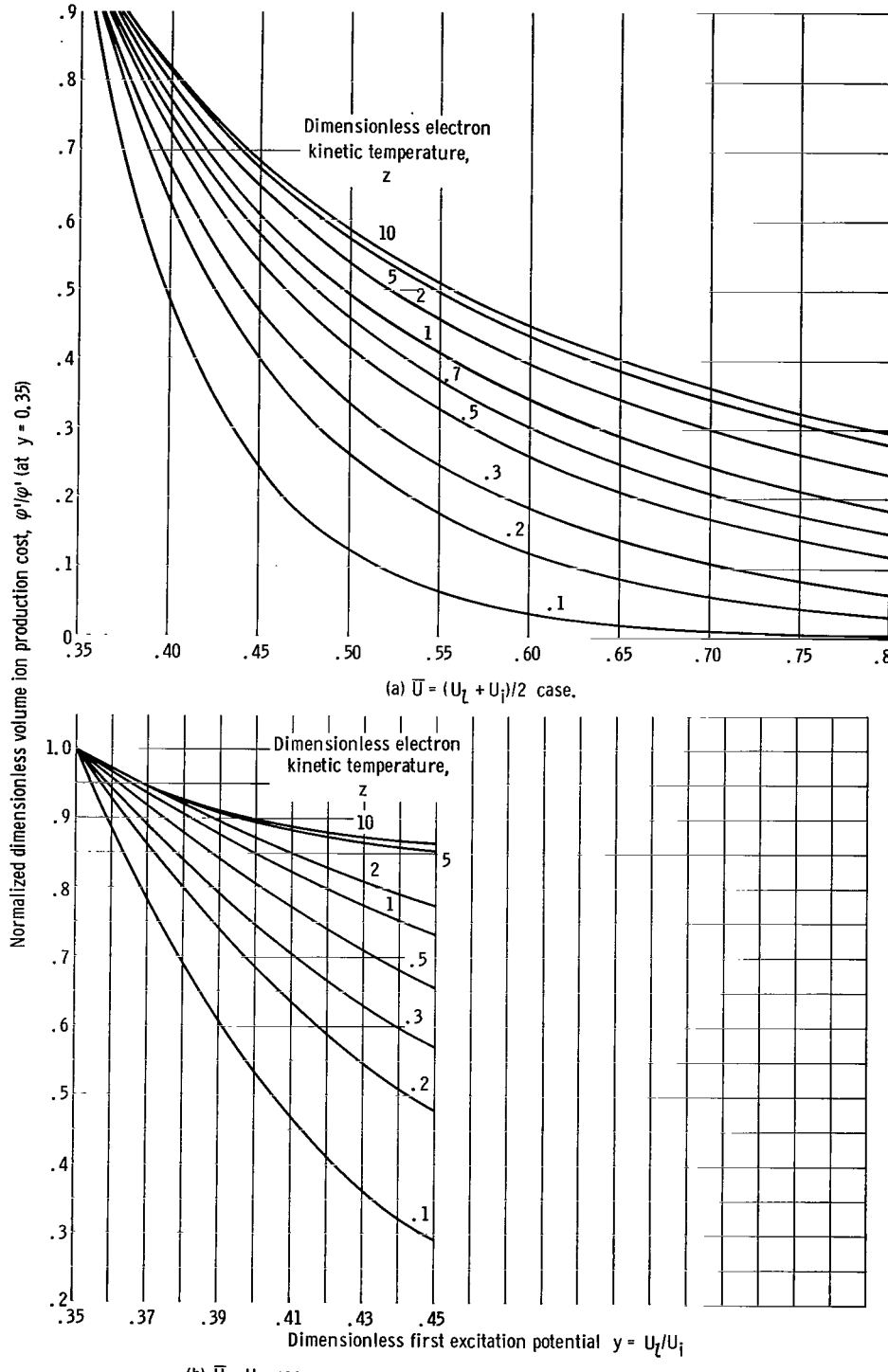


Figure 22. - Normalized dimensionless volume ion production cost $\varphi'/\varphi'$ (at $y = 0.35$) plotted against dimensionless first excitation potential $y = U_l/U_i$ with dimensionless electron kinetic temperature $z = kT_e/U_i$ as parameter.

*"The aeronautical and space activities of the United States shall be conducted so as to contribute . . . to the expansion of human knowledge of phenomena in the atmosphere and space. The Administration shall provide for the widest practicable and appropriate dissemination of information concerning its activities and the results thereof."*

—NATIONAL AERONAUTICS AND SPACE ACT OF 1958

# NASA SCIENTIFIC AND TECHNICAL PUBLICATIONS

TECHNICAL REPORTS: Scientific and technical information considered important, complete, and a lasting contribution to existing knowledge.

TECHNICAL NOTES: Information less broad in scope but nevertheless of importance as a contribution to existing knowledge.

TECHNICAL MEMORANDUMS: Information receiving limited distribution because of preliminary data, security classification, or other reasons.

CONTRACTOR REPORTS: Scientific and technical information generated under a NASA contract or grant and considered an important contribution to existing knowledge.

TECHNICAL TRANSLATIONS: Information published in a foreign language considered to merit NASA distribution in English.

SPECIAL PUBLICATIONS: Information derived from or of value to NASA activities. Publications include conference proceedings, monographs, data compilations, handbooks, sourcebooks, and special bibliographies.

TECHNOLOGY UTILIZATION PUBLICATIONS: Information on technology used by NASA that may be of particular interest in commercial and other non-aerospace applications. Publications include Tech Briefs, Technology Utilization Reports and Notes, and Technology Surveys.

***Details on the availability of these publications may be obtained from:***

SCIENTIFIC AND TECHNICAL INFORMATION DIVISION

NATIONAL AERONAUTICS AND SPACE ADMINISTRATION

**Washington, D.C. 20546**